



**HAL**  
open science

## **Delineating the Physiological Roles of the PE and Catalytic Domains of LipY in Lipid Consumption in Mycobacterium-Infected Foamy Macrophages**

Pierre Santucci, Sadia Diomandé, Isabelle Poncin, Laetitia Alibaud, Albertus Viljoen, Laurent Kremer, Chantal de Chastellier, Stéphane Canaan

► **To cite this version:**

Pierre Santucci, Sadia Diomandé, Isabelle Poncin, Laetitia Alibaud, Albertus Viljoen, et al.. Delineating the Physiological Roles of the PE and Catalytic Domains of LipY in Lipid Consumption in Mycobacterium-Infected Foamy Macrophages. *Infection and Immunity*, 2018, 86 (9), 10.1128/IAI.00394-18 . hal-01860679

**HAL Id: hal-01860679**

**<https://amu.hal.science/hal-01860679>**

Submitted on 23 Aug 2018

**HAL** is a multi-disciplinary open access archive for the deposit and dissemination of scientific research documents, whether they are published or not. The documents may come from teaching and research institutions in France or abroad, or from public or private research centers.

L'archive ouverte pluridisciplinaire **HAL**, est destinée au dépôt et à la diffusion de documents scientifiques de niveau recherche, publiés ou non, émanant des établissements d'enseignement et de recherche français ou étrangers, des laboratoires publics ou privés.

1 **Delineating the physiological roles of the PE and catalytic domain of LipY in lipid**  
2 **consumption in mycobacteria-infected foamy macrophages**

3 Pierre Santucci<sup>§</sup>, Sadia Diomandé<sup>§</sup>, Isabelle Poncin<sup>§</sup>, Laetitia Alibaud<sup>‡</sup>, Albertus  
4 Viljoen<sup>¶</sup>, Laurent Kremer<sup>†,¶</sup>, Chantal de Chastellier<sup>!,\*</sup> and Stéphane Canaan<sup>§\*</sup>

5

6 <sup>§</sup>Aix-Marseille Univ, CNRS, LISM, IMM FR3479, Marseille, France.

7 <sup>!</sup>Centre d'Immunologie de Marseille-Luminy, Aix Marseille Université UM2, Inserm,  
8 U1104, CNRS UMR7280, Marseille, 13288, France

9 <sup>‡</sup>CNRS UMR5235, Université de Montpellier, Montpellier, France

10 <sup>¶</sup>Institut de Recherche en Infectiologie de Montpellier (IRIM), Université de  
11 Montpellier, CNRS UMR9004, Montpellier, France.

12 <sup>†</sup>INSERM, IRIM, Montpellier, France.

13

14

15

16

17

18 **Running title:** Contribution of the LipY PE domain to lipid hydrolysis.

19

20 **Keywords:** Electron microscopy, lipolysis, lipid bodies, intracytosolic lipid inclusions,  
21 *Mycobacterium tuberculosis*, *M. bovis* BCG.

22

23 **\*Corresponding authors:** Chantal de Chastellier, (chantal.[dechastellier@wanadoo.fr](mailto:dechastellier@wanadoo.fr))  
24 and Stéphane Canaan (canaan@imm.cnrs.fr).

25

26 **ABSTRACT**

27 Within tuberculous granulomas, a sub-population of *Mycobacterium tuberculosis*  
28 resides inside foamy macrophages (FM) that contain abundant cytoplasmic lipid  
29 bodies (LB) filled with triacylglycerol (TAG). Upon fusion of LB with *M. tuberculosis*-  
30 containing phagosomes, TAG is hydrolyzed and reprocessed by the bacteria into their  
31 own lipids, which accumulate as intracytosolic lipid inclusions (ILI). This phenomenon  
32 is driven by many mycobacterial lipases, among which LipY participates in the  
33 hydrolysis of host and bacterial TAG. However, the functional contribution of LipY's PE  
34 domain in TAG hydrolysis remains unclear. Herein, enzymatic studies were performed  
35 to compare the lipolytic activity of recombinant LipY and its truncated variant lacking  
36 the N-terminal PE domain, LipY( $\Delta$ PE). Complementarily, an FM model was used  
37 where BMDM were infected with *M. bovis* BCG strains either overexpressing LipY or  
38 LipY( $\Delta$ PE) or carrying a *lipY*-deletion mutation prior to being exposed to TAG-rich  
39 VLDL. Results indicate that truncation of the PE domain correlates with increased TAG  
40 hydrolase activity. Quantitative electron microscopy analyses showed that (i) in the  
41 presence of lipase inhibitors, large ILI were not formed either because of an absence  
42 of LB due to inhibition of VLDL-TAG hydrolysis or inhibition of LB-neutral lipid  
43 hydrolysis by mycobacterial lipases; (ii) large ILI<sup>+3</sup> in the strain overexpressing  
44 LipY( $\Delta$ PE) were reduced and, (iii) the number of ILI<sup>+3</sup> profiles in the  $\Delta$ *lipY* mutant was  
45 reduced by 50%. Overall, these results delineate the role of LipY and its PE domain in  
46 host and mycobacterial lipid consumption and show that additional mycobacterial  
47 lipases take part in these processes.

48

## 49 INTRODUCTION

50 With more than 10 million new cases and 1.7 million deaths in 2016, tuberculosis  
51 (TB), caused by *Mycobacterium tuberculosis*, remains one of the most devastating  
52 diseases worldwide (1). This serious illness is not fully treatable with current medication.  
53 Prognosis of the disease depends on the host's ability to contain the bacilli at the site of  
54 infection within granulomas. Tuberculous granulomas are complex and dynamic  
55 immunological structures, which generate a wide range of microenvironments (2, 3) that  
56 are assumed to drastically affect the tubercle bacilli physiological properties (3, 4). Inside  
57 the high diversity of TB pulmonary lesions found during active disease or latent infection,  
58 a distinct bacterial sub-population appears associated with a specific cell type consisting  
59 of foamy macrophages (FM) characterized by the presence of numerous triacylglycerol  
60 (TAG)-filled lipid bodies (LB) in their cytosol (2, 5, 6). To date, the exact role of FM in TB  
61 pathogenesis remains elusive, however these specialized lipid-rich cells have been  
62 described in both experimentally-infected animals and patients suggesting that they might  
63 play an essential role in granuloma formation and maturation processes. Several  
64 independent studies have demonstrated that pathogenic mycobacteria during *in-vitro* FM  
65 infection, are able to survive in a slow or non-replicating state (5, 7). These experimental  
66 observations prompted the authors to propose that FM may also promote *M. tb*  
67 intracellular survival for extensive periods *in vivo*, although this remains to be  
68 demonstrated. A better understanding of how mycobacteria interact with and persist  
69 within FM is important to decipher this complex host-pathogen crosstalk that may sustain  
70 latent TB and, eventually, to identify new pharmacological approaches to control both  
71 active and latent TB. It is well-known that storage of large amounts of neutral lipids in the  
72 form of intracytosolic lipid inclusions (ILI) is one of the main characteristics of persistent  
73 mycobacteria (8). ILI are mainly composed of triacylglycerols (TAG) resynthesized by

74 mycobacterial TAG synthases from free fatty acids coming from the hydrolysis of host  
75 TAG (9-12). Host lipid transfer to the phagosomal lumen occurs *via* mycobacterium-  
76 induced fusion between LB and phagosomes (7). Lipids within ILI seem to serve as a  
77 source of carbon and energy prior to reactivation of dormant bacilli (11, 13).

78         Although the origin of the ILI-containing lipids has become the focus of intense  
79 research (5, 10, 11, 14, 15), the catalytic steps involved in the formation of mycobacterial  
80 ILI are not completely understood (16, 17). It is obvious, however, that hydrolysis of host  
81 TAG released into the phagosome involves specific mycobacterial lipolytic enzymes,  
82 either secreted by the bacilli into the phagosomal lumen or associated with the outermost  
83 layer of the mycobacterial cell wall (16, 18-20) whereas lipolytic enzymes involved in  
84 hydrolysis of ILI-contained TAG must be located in the mycobacterial cytosol (11, 21, 22).  
85 Among the many mycobacterial lipases found in *M. tuberculosis*, LipY (Rv3097c) appears  
86 as a major player in the degradation of TAG within ILI under *in vitro* growth conditions  
87 mimicking dormancy (11, 21, 22). LipY belongs to the hormone-sensitive lipase family  
88 and displays an N-terminal PE domain that is specific to pathogenic mycobacterial  
89 species (21-23). Relevant studies demonstrated that PE proteins are exported to the cell  
90 wall *via* the type VII secretion system ESX-5 after recognition of the specific amino-acid  
91 sequence YxxxD/E contained in the N-terminal PE domain (18, 24-26). Among the  
92 enzymes of the PE family, only two members, PE-PGRS11 (or Rv0754), a functional  
93 phosphoglycerate mutase (27) and LipY, have been biochemically characterized. LipY  
94 was proposed to be a major contributor to the breakdown of stored TAG (21, 22). In  
95 addition, a recombinant *Mycobacterium smegmatis* strain overexpressing the full-length  
96 LipY, exhibited a reduced TAG hydrolytic activity as compared to a LipY variant shortened  
97 by its N-terminal PE domain, LipY( $\Delta$ PE), suggesting that the PE domain may negatively  
98 modulate the activity of LipY (22, 28).

99 In the present study, the experimental model system of VLDL-driven FM (7) was  
100 used to delineate the physiological role of the PE domain of LipY in the hydrolysis of both  
101 host-derived TAG and mycobacterial TAG within ILI. Reasons for choosing this model  
102 system have been described in detail elsewhere (7, 12, 14, 29). After internalization of  
103 VLDL by receptor-mediated endocytosis, the neutral lipids of this lipoprotein will undergo  
104 hydrolysis in lysosomes. This will provide fatty acids for the subsequent biosynthesis of  
105 neutral lipids, including TAG, between the two leaflets of the endoplasmic reticulum,  
106 where LB, consisting of a phospholipid monolayer encapsulating neutral lipids, bud of.  
107 This model system generates defined conditions for inducing the formation or removal of  
108 LB, which triggers ILI formation or consumption, and helps delineating the role of host cell  
109 or mycobacterial lipases in these processes.

110 We first show that addition of lipase inhibitors, during exposure of infected cells to  
111 VLDL, inhibits the accumulation of lipids in the form of ILI by affecting either the  
112 macrophage lysosomal TAG hydrolase and, hence, LB formation, or mycobacterial  
113 lipases involved in the hydrolysis of host TAG delivered to phagosomes. Next, we  
114 demonstrate the modulatory role of its N-terminal PE domain on LipY function by, as a  
115 first approach, comparing the catalytic activity of purified LipY and LipY( $\Delta$ PE) variants  
116 using a range of lipids with various chain lengths. As a second approach, we used  
117 quantitative electron microscopy (EM) methods to examine differences in mycobacterial  
118 ILI formation in bone marrow-derived mouse macrophages (BMDM) exposed to VLDL to  
119 become foamy after they were infected with *M. bovis* BCG strains overexpressing  
120 different LipY variants or in which the *lipY* gene was deleted. This study indicates that  
121 other lipases, in addition to LipY, are likely to be involved in ILI formation. Removal of  
122 VLDL normally leads to the loss of TAG-containing ILI (7). When lipase inhibitors were

123 added after exposure to VLDL no loss of ILI occurred, a result that emphasizes the  
124 participation of several lipolytic enzymes in the hydrolysis of bacterial cytosolic TAG.

125

126 **MATERIALS AND METHODS**

127 **Reagents.** DMEM and glutaraldehyde grade I (EM grade) were purchased from Sigma  
128 (St Louis, MO, USA), FBS was from Biowest (Nuaille, France), PBS was from GIBCO  
129 (distributed by Invitrogen, Villebon sur Yvette, France), commercial Very Low Density  
130 Lipoprotein (VLDL) was from Calbiochem-Merck (Darmstadt, Germany), osmium  
131 tetroxide and Spurr resin were from Electron Microscopy Sciences (distributed by  
132 Euromedex, Mundolsheim, France). All bacterial culture media were purchased from Life  
133 technologies (USA).

134

135 **Bacterial strains and growth conditions.** *Escherichia coli* DH10B cells (Invitrogen)  
136 used in cloning experiments were grown at 37°C in Luria Bertani (LB) broth (Invitrogen)  
137 or on LB agar plates. Culture media were supplemented with 200 µg/mL hygromycin B.  
138 The *M. smegmatis* mc<sup>2</sup>155 *groEL1ΔC* strain (30) used for expression experiments was  
139 routinely grown at 37°C with shaking (220 rpm) in Middlebrook 7H9 medium (Difco)  
140 supplemented with 0.05% Tween 80 (v/v), 0.2% glycerol (v/v), 0.5% bovine serum  
141 albumin (BSA) (w/v) and 0.2% glucose (w/v) or on Middlebrook 7H11 (Difco) agar plates.  
142 The *M. bovis* BCG Pasteur 1173P2 strain used for overexpression experiments was  
143 grown at 37°C with shaking (160 rpm) in Middlebrook 7H9 medium supplemented with  
144 0.05% Tween 80 (v/v), 0.2% glycerol (v/v) and 10% Albumin Dextrose Catalase (v/v)  
145 (ADC). Preparation of *M. smegmatis* and *M. bovis* BCG electrocompetent cells and  
146 electroporation procedures were performed as described previously (31). Transformants  
147 were selected on Middlebrook 7H11 agar supplemented with 10% ADC and either  
148 50 µg/mL hygromycin or 50 µg/mL kanamycin. Plates were incubated at 37°C for 3-5  
149 days for *M. smegmatis* and for three weeks for *M. bovis* BCG.

150

151 **Complementation of *M. bovis* BCG  $\Delta lipY$  strain.** A *M. bovis* BCG mutant lacking the  
152 *lipY* gene ( $\Delta lipY$ ) was grown in the presence of 50  $\mu\text{g}/\text{mL}$  hygromycin (32).  
153 Complementation was performed by introducing pMV261::*lipY* (22) prior to selection on  
154 7H11 Middlebrook agar medium supplemented with 10% ADC and kanamycin. Presence  
155 of the plasmid was checked by PCR and expression of LipY confirmed by immunoblotting.  
156 Briefly, bacterial lysates from the WT,  $\Delta lipY$  and complemented strain ( $\Delta lipY::Comp$ ) were  
157 normalized for total protein content, electrophoretically separated on a 12% SDS-PAGE  
158 gel and transferred onto a nitrocellulose membrane using a Trans-Blot Turbo Transfer  
159 System (Bio-Rad). Membranes were then saturated with 1% bovine serum albumin (BSA)  
160 in PBS, 0.1% Tween 20 and probed for 1 hour with mouse antiserum raised against LipY  
161 at a 1/2,500 dilution. After extensive washing, the membrane was incubated with  
162 horseradish peroxidase-conjugated IgG anti-mouse antibodies (Sigma-Aldrich). The  
163 GroEL2 protein was used as protein loading control and was revealed using the  
164 HisProbe<sup>TM</sup> HRP conjugate (Thermo-Scientific) which recognizes the natural poly-  
165 Histidine sequence present in its C-terminal domain (33, 34). Detection was achieved  
166 using the Pierce<sup>TM</sup> ECL Western Blotting substrate solution (Thermo-Scientific) and  
167 visualized using the ChemiDoc<sup>TM</sup> MP Imaging System (Bio-Rad).

168  
169 **Cloning, expression and purification of LipY and LipY( $\Delta PE$ ).** The *lipY* and *lipY( $\Delta PE$ )*  
170 genes were amplified by PCR using *M. tuberculosis* H37Rv genomic DNA and cloned  
171 into pSD26 under the control of the acetamide inducible promoter and carrying a  
172 hygromycin resistance cassette (35) or into pMV261 (36) downstream of the *hsp60*  
173 promoter and containing a kanamycin resistance cassette, as reported previously (22).  
174 DNA sequence analysis of each insert was performed by GATC Biotech (Germany).

175 Expression and purification of recombinant LipY or LipY( $\Delta$ PE) were performed as  
176 previously reported (37) with some minor modifications. Briefly, *M. smegmatis* mc<sup>2</sup>155  
177 *groEL1* $\Delta$ C strains carrying pSD26-*lipY* and pSD26-*lipY*( $\Delta$ PE), were used to inoculate 10  
178 mL of 7H9 medium containing 50  $\mu$ g/mL hygromycin. After three days of incubation at  
179 37°C with shaking, 10 mL of the preparation were used to inoculate 400 mL of culture  
180 medium for a large-scale production. Cultures were grown at 37°C with shaking (220 rpm)  
181 until an OD<sub>600nm</sub> value between 2.5 and 3 was reached. Expression of recombinant  
182 proteins was induced by adding acetamide to a final concentration of 0.2% (w/v) for 16 h.  
183 Bacteria were harvested, resuspended in ice-cold buffer A (10 mM Tris/HCl pH 8.0,  
184 150 mM NaCl) (30 mL) containing 1% *N*-lauroylsarcosine and lysed using a French Press  
185 set 1100 psi. After centrifugation, the supernatant (S1) was recovered while the resulting  
186 pellet was resuspended in buffer A (30 mL) and sonicated twice for 30 s with 30 s breaks  
187 between each cycle and stirred overnight at 4°C. After centrifugation, the new  
188 supernatant (S2) was pooled with S1 supernatant and the mixture was loaded onto a Ni<sup>2+</sup>-  
189 NTA resin equilibrated with buffer A. The column was subsequently washed with buffer A  
190 without detergent prior to elution with increasing concentrations of imidazole. The eluted  
191 fractions were analysed by performing 12% SDS-PAGE as described previously (38).  
192 Fractions containing pure proteins were pooled, dialysed overnight against buffer A and  
193 concentrated by ultrafiltration to a final concentration of 0.6 mg/mL and stored at -80°C.  
194 Theoretical physical properties (molecular mass, extinction coefficient at 280 nm and  
195 isoelectric point) of both proteins containing the His<sub>6</sub>-tag at the C-Terminal position were  
196 obtained from the ProtParam tool (<http://ca.expasy.org/tools/protparam.html>).

197

198 **Enzyme activity measurements using the pH-stat technique.** Enzymatic hydrolysis of  
199 emulsions of mono-, di- and triacylglycerol namely monobutylin (MC4), monolein (MC18),

200 diolein (DC18), tributyrin (TC4) and trioctanoin (TC8) were monitored titrimetrically for at  
201 least 5 min at 37°C using a pH-stat (Metrohm 718 STAT Titrino; Metrohm Ltd., Herisau,  
202 Switzerland). Assays were performed in 2.5 mM Tris-HCl buffer (pH 7.5) containing 300  
203 mM NaCl and 3 mM NaTDC (23, 39). Free fatty acids released were automatically titrated  
204 with 0.1 M NaOH to maintain a fixed end-point pH value of 7.5. The specific activity of  
205 both enzymes was expressed in units per mg of pure enzyme. One unit corresponds to  
206 the release of 1  $\mu$ mole of fatty acid per minute.

207  
208 **Lipase activity assays on TAG from Pomegranate oil.** Corning UV 96-well microplates  
209 were coated as recently described (40) using TAG from Pomegranate oil, containing up  
210 to 80% punicic acid (C18:3) equally present at the 3 positions of the glycerol backbone.  
211 The lipase activity was measured at 37°C in 10 mM Tris-HCl buffer (pH 7.5) containing  
212 150 mM NaCl, 6 mM CaCl<sub>2</sub>, 1 mM EDTA, 0.001% (w/v) 3,5-di-*tert*-4-butylhydroxytoluene  
213 (BHT) and 3 mg/mL  $\beta$ -Cyclodextrine ( $\beta$ -CD). The formation of the  $\beta$ -CD/free punicic acid  
214 complex was continuously monitored at 275 nm for 60 min.

215  
216 ***In silico* Protein Modeling.** Three-dimensional structural models of LipY and LipY( $\Delta$ PE)  
217 proteins were generated with the automatic protein structure homology modeling server  
218 using the I-Tasser software program (41, 42). The alignment of the LipY and LipY $\Delta$ PE  
219 sequences were performed using Multalin multiple sequence alignment (43) and the  
220 result was displayed with ESPript (44). The structural overlay and figures were drawn  
221 using the PyMOL Molecular Graphics System (version 1.8.6.0, Schrödinger, LLC).

222  
223 **Infection of bone marrow-derived mouse macrophages (BMDM) with recombinant**  
224 ***M. bovis* BCG strains.** Bone marrow cells were isolated from the femurs of 6- to 8-week-

225 old C57BL/6 female mice and seeded onto tissue culture dishes (Falcon; Becton  
226 Dickinson Labware, Meylan, France) 35 mm in diameter ( $4 \times 10^5$  cells per dish). The  
227 culture medium was DMEM with high glucose ( $1 \text{ g liter}^{-1}$ ) and high carbonate ( $3.7 \text{ g liter}^{-1}$ )  
228 <sup>1</sup>) concentrations supplemented with 10% heat-inactivated FBS, 10% L-cell conditioned  
229 medium (a source of colony-stimulating factor 1, CSF-1), and 2 mM L-glutamine. Five  
230 days after seeding, the adherent cells were washed twice with DMEM and refed with  
231 complete medium. Medium was then renewed on day 6. No antibiotics were added. On  
232 day 7, the cells were infected for 4 h at  $37^\circ\text{C}$  with wild type or different recombinant *M.*  
233 *bovis* BCG strains at a multiplicity of infection (MOI) of 5 for EM studies, washed in 4  
234 changes of ice-cold PBS to eliminate non-ingested bacteria, and further incubated in  
235 complete medium devoid of antibiotics. For long-term cultures, the medium was changed  
236 twice a week.

237  
238 **Treatment with VLDL and chase after treatment.** After active replication of *M. bovis*  
239 BCG for 6 days, infected macrophages were exposed to Very Low Density Lipoprotein  
240 (VLDL), for 24 h. The volume of VLDL was adjusted so as to expose cells ( $1 \times 10^6$  per  
241 dish) to  $180 \mu\text{g TAG}$  per mL of medium. In some instances, infected cells were exposed  
242 to VLDL simultaneously with either tetrahydrolipstatin (THL also named Orlistat,  $60 \mu\text{g/mL}$   
243 in ethanol) or *MmPPOX* ( $15 \mu\text{g/mL}$  in ethanol) for 24 h (23). Cells were also exposed to  
244 VLDL for 24 h, washed and incubated in a VLDL-free fresh medium with or without THL  
245 or *MmPPOX* for 24 h.

246  
247 **Processing for conventional electron microscopy (EM).** Cells were fixed for 1 h at  
248 room temperature with 2.5% glutaraldehyde in 0.1 M sodium cacodylate buffer (pH 7.2)  
249 containing 0.1 M sucrose, 5 mM  $\text{CaCl}_2$ , and 5 mM  $\text{MgCl}_2$ , washed with complete

250 cacodylate buffer, and post-fixed for 1 h at room temperature with 1% osmium tetroxide  
251 in the same buffer devoid of sucrose. They were washed with buffer, scraped off the  
252 dishes, concentrated in 2% agar in cacodylate buffer, and treated for 1 h at room  
253 temperature with 1% uranyl acetate in 30% methanol. Samples were dehydrated in a  
254 graded series of ethanol solutions and embedded in Spurr resin. Thin sections (70 nm  
255 thick) were stained with 1% uranyl acetate in distilled water and then with lead citrate.

256  
257 **Quantification and statistical analysis.** At the time points indicated in the figures, 150  
258 to 300 intraphagosomal mycobacteria per sample were examined under an EM to score  
259 the percentage of each category of *M. bovis* BCG ILI profiles. The cells were examined  
260 at random, and care was taken to avoid serial sections. Histograms represent the mean  
261  $\pm$  standard deviation of at least three independent counts. Statistical analyses were  
262 performed using GraphPad Prism 4.03 and differences were considered statistically  
263 significant when *P*-values were  $\leq 0.05$  using two tailed Student's *t*-tests.

264

265 **RESULTS**

266 **ILI formation depends on lipid processing by macrophage and mycobacterial**  
267 **lipases.** Previously, we have shown the dependence of ILI formation on the presence of  
268 LB in the host, confirmed the finding that host TAG provided the bulk of lipid for ILI  
269 formation and demonstrated that VLDL-derived TAG must first be processed by host  
270 lysosomal lipases (7). The requirement of host lipases for the release of fatty acids had  
271 been tested by exposing *M. avium*-infected macrophages for 24 h to VLDL in the  
272 presence of the anti-obesity drug, tetrahydrolipstatin (THL or Orlistat®). THL inhibits  
273 human digestive lipases within the gastro-intestinal tract (45) as well as a variety of other  
274 serine-hydrolases (46, 47), including mycobacterial LipY, a major enzyme responsible for  
275 hydrolysis of ILI-contained TAG (21).

276 In the present work, we applied the above procedure to cells infected with wild-  
277 type *M. bovis* BCG. As described in our previous study (7), endocytosis of VLDL and  
278 transfer to lysosomes was not affected by THL but TAG and derivatives in VLDL were not  
279 degraded as usual. These lipids were easily recognized by their electron-transparency  
280 and were seen to fill the entire lumen of most lysosomes, leaving only small spaces with  
281 the usual electron-dense lysosomal contents (Fig. 1A). This was not observed when  
282 infected cells were exposed to VLDL only, in which case lysosomes keep their normal  
283 electron-dense appearance (Fig. 1B). In the presence of THL, very few, if any, LB were  
284 observed with an average value of approximately 0.32 LB per cell (Supplemental Material,  
285 Fig. S1). As expected, with this extremely low level of LB (approximately 23 times less  
286 than the untreated cells), mycobacterial profiles with large ILI filling most of the  
287 mycobacterial cytoplasm (defined as ILI<sup>+3</sup> in (7)) were infrequent (Fig. 1C) as opposed to  
288 when LB were formed in the presence of VLDL only (Fig 1D). A quantitative evaluation  
289 (Fig. 1G) showed that the amount of ILI<sup>+3</sup> and ILI<sup>+2</sup> profiles remained low, less than 1%

290 and 23%  $\pm$ 1.1, respectively, in presence of THL vs 25%  $\pm$  7.4 and 45%  $\pm$  2, respectively,  
291 in the absence of this lipase inhibitor. Consequently, the amount of ILI<sup>(+1/-)</sup> profiles was  
292 2.5 fold higher in presence of THL (with: 78%  $\pm$  9.6; without: 31%  $\pm$  0.5).

293 These results suggest that mycobacterial lipases were unable to process TAG in  
294 the VLDL core directly and that VLDL-derived TAG first had to be processed by lysosomal  
295 lipases in order to hydrolyze TAG into diacylglycerides (DAG) and monoacylglycerides  
296 (MAG) and FFA for subsequent re-processing into TAG and accumulation in LB. Because  
297 no LB were formed, it was not possible to gain information on the role of mycobacterial  
298 lipases on host TAG hydrolysis. However, THL has also been reported as a non-specific  
299 inhibitor of a wide range of serine-hydrolases from both mammals and bacterial species  
300 (13, 19, 48, 49) and, therefore one cannot exclude that mycobacterial enzymes are also  
301 inhibited by THL, thereby impacting ILI formation.

302 We then resorted to the oxadiazolone inhibitor, *MmPPOX*, known to inhibit a  
303 variety of mycobacterial serine-hydrolases including those of the hormone-sensitive  
304 lipase (HSL) family (50), and more specifically LipY (18, 23). After exposure of *M. bovis*  
305 BCG-infected cells to VLDL in the presence of *MmPPOX*, host lysosomes were not  
306 affected in the same way as during THL treatment. Here, most lysosomes retained their  
307 usual electron-dense appearance. Less than 25% of the lysosomes contained small lipid  
308 droplets (Fig. 1E) and only 10% were filled with TAG and derivatives as in the case of  
309 macrophages exposed to VLDL with THL. Notably, with *MmPPOX* the relative number of  
310 LB per cell was 6 to 7 times higher than with a THL treatment (Supplemental Material,  
311 Fig. S1), with an average value of 2.1 LB per cell (thus leading to a 3.5-fold reduction in  
312 LB content, in comparison with an untreated sample). These data suggest that host  
313 lysosomal lipases were poorly affected by *MmPPOX*. As a result, VLDL-derived TAG

314 could be broken down into di- and mono-glycerides and fatty acids for re-processing into  
315 TAG and accumulation in LB.

316 Strikingly, during *MmPPOX* treatment mycobacterial profiles with large ILI were  
317 not observed as demonstrated (Fig. 1F). A quantitative evaluation of mycobacterial  
318 profiles containing the different categories of ILI showed that those with large (ILI<sup>+3</sup>) and  
319 medium-sized (ILI<sup>+2</sup>) ILI reached less than 5% and 20%, respectively, of the amount  
320 generated by cell exposure to VLDL in absence of *MmPPOX* (Fig. 1G). These data  
321 suggest that the cell-surface exposed mycobacterial lipases involved in hydrolysis of host  
322 TAG delivered to wild-type *M. bovis* BCG-containing phagosomes are involved in ILI  
323 formation and that *MmPPOX* appears to inhibit the mycobacterial lipases more efficiently  
324 than THL. By comparing the LB/ILI relative ratio from the two treated samples, a clear  
325 difference in the effects of the two inhibitors was observed where LB/ILI<sup>+3</sup> and LB/ILI<sup>+2</sup>  
326 ratios were 9.8 and 12.4 times higher, respectively, in *MmPPOX* than in THL treated  
327 samples (Supplemental Material, Fig. S1).

328 Altogether, these data further support that in our system, VLDL has to be  
329 processed by host lipases in order to newly synthesize host LB, and that these neutral  
330 lipid-rich organelles have to be delivered within mycobacteria-containing phagosomes for  
331 subsequent hydrolysis into free fatty acids, which will allow ILI formation. However, these  
332 experiments do not allow to identify specific mycobacterial lipase(s) involved in this  
333 process, although the LipY form associated with the mycobacterial surface remains the  
334 most likely candidate.

335  
336 **Biochemical characterization of rLipY and rLipY( $\Delta$ PE).** The LipY hydrolase from  
337 *M. tuberculosis* has a dual location, firstly in the mycobacterial cytosol where it has direct  
338 access to ILI for subsequent lipid hydrolysis (21, 22) and, second, at the mycobacterial

339 cell surface in a truncated/mature form following removal of its N-terminal PE domain (18,  
340 21, 22, 51). This dual localization has been explained by Daleke *et al.* (18) who  
341 demonstrated that the PE domain of LipY is essential for secretion by ESX-5 (18, 25, 26).  
342 It is not known, however, whether this secretion also requires additional partners such as  
343 PPE proteins, which are known to form pairs with PE proteins. Mishra *et al.* proposed that  
344 the PE domain not only plays a role in the recognition by ESX-5 for secretion of LipY but  
345 also contributes to the enzymatic activity of the protein (22). Overexpression of  
346 LipY( $\Delta$ PE), a LipY version lacking its N-terminal PE domain, in *M. smegmatis* was  
347 associated with increased activity as compared to the strain overexpressing the full-length  
348 protein (22). Nevertheless, whether lack of the PE domain directly affects LipY activity or  
349 whether the increased activity of LipY( $\Delta$ PE) results from an indirect effect, presumably  
350 due to the absence of a possible partner, remains unknown. To address this issue, we  
351 compared the enzymatic activity of purified LipY and LipY( $\Delta$ PE) recombinant proteins.

352 Because the *E. coli* expression system failed to express large amounts of LipY in an  
353 active form, we opted for *M. smegmatis* mc<sup>2</sup>155 *groEL1* $\Delta$ C as a surrogate host which  
354 allowed producing around 30 mg of pure and active recombinant LipY from a 400 mL  
355 culture volume (Fig. 2A). Regarding rLipY( $\Delta$ PE), 9 mg of pure (Fig. 2A) and active  
356 enzyme were obtained from equivalent cultures, thus indicating that the PE domain is not  
357 needed for proper folding of the protein. This was confirmed by further biochemical  
358 analyses and circular dichroism spectra determination of both recombinant enzymes  
359 (data not shown). The lower rLipY( $\Delta$ PE) yield could rely on the absence of the PE domain  
360 that exposes the lipid binding site of LipY, promoting a higher degree of interactions  
361 between molecules and excessive protein aggregation.

362 The specific activity of rLipY and rLipY( $\Delta$ PE) was determined using a range of lipid  
363 substrates differing in their chain lengths and by combining titrimetric and

364 spectrophotometric techniques. Regardless of the lipid substrates used, rLipY( $\Delta$ PE)  
365 exhibited higher specific activities (1.2 to 2.5 times depending on the substrate) than rLipY  
366 (Table 1). Both proteins were preferentially active on short-chain emulsified MAG and  
367 TAG, i.e., monobutylin ( $61.0 \pm 2.0$  and  $92.0 \pm 5.0$  U/mg, respectively) and tributyrin ( $129.0$   
368  $\pm 6.0$  and  $267.0 \pm 24.0$  U/mg, respectively) and displayed the same chain length  
369 specificity since their respective specific activities decreased gradually as the substrate  
370 chain length increased (Table 1). These results unambiguously show that the lipase  
371 activity of LipY is significantly enhanced in the absence of its PE domain, consistent with  
372 previous findings (22). Moreover, LipY has a nonspecific lipase activity able to hydrolyse  
373 DAG and MAG as well as TAG. Therefore, LipY has the potential to degrade total host  
374 TAG converting them into glycerol and free fatty acids, products that can subsequently  
375 be directly absorbed by the bacteria.

376 The N-terminus contains 4  $\alpha$ -helices ( $\alpha 1$  to  $\alpha 4$ ), all lacking in LipY( $\Delta$ PE) (Fig. 2B).  
377 Molecular modelling was performed allowing us to propose the overall structures of both  
378 the full-length and the truncated LipY proteins (Fig. 2C) and to address whether these  
379 secondary structures may alter either the optimal recognition and/or binding of the  
380 substrates to LipY. The  $\alpha 1$ - $\alpha 4$  helices of the PE domain are connected to a linker unit  
381 composed of three helices ( $\alpha 5$ - $\alpha 7$ ), presumably providing a high degree of flexibility to  
382 the PE and core (C-terminal) domains. The latter, comprising the active site of LipY  
383 belongs to the  $\alpha/\beta$  hydrolase fold family and is composed of a central  $\beta$ -sheet ( $\beta 1$ - $\beta 8$   
384 strands) surrounded by nine  $\alpha$ -helices. Similar to most lipases, the catalytic serine  
385 (Ser309) is located in a nucleophile elbow between the  $\beta 5$  strand and the  $\alpha 13$  helix. The  
386 presence of the PE domain (Fig. 2C) clearly reduces the accessibility of the active site to  
387 the substrate. Removal of the PE domain allows the linker portion (green) to move to the  
388 side of the catalytic domain, thus opening access to the active site. This large opening

389 presumably allows a better accommodation of the lipid substrates into the active site,  
390 thereby contributing to the increased enzymatic activity of LipY( $\Delta$ PE).

391  
392 **Distribution of ILI profiles in *M. bovis* BCG strains over-expressing various LipY**  
393 **variants in VLDL-driven FM.** To investigate the functional contribution of the PE domain  
394 of LipY in host TAG hydrolysis and consequently ILI formation, macrophages were  
395 infected with various *M. bovis* BCG strains for 6 days, before being exposed to VLDL for  
396 24 h to induce FM formation (7). The strains used in this experiment were the wild-type  
397 BCG strain (WT), which is characterized by the native expression of LipY and was used  
398 as reference, and three other recombinant BCG strains harboring distinct pMV261-  
399 derived constructs, leading to the overproduction of either LipY, LipY( $\Delta$ PE) or LipY( $\Delta$ PE)  
400 in which Ser309 was replaced by an Ala residue (LipY( $\Delta$ PE)<sup>S309A</sup>) yielding a catalytically-  
401 inactive protein (22). Cells were then fixed and processed for EM and profiles of  
402 intracellular mycobacteria were examined for the presence and extent of ILI formation in  
403 both VLDL-treated and untreated macrophages. As before (7), intracellular mycobacteria  
404 were divided into 4 categories according to their ILI size (Figs. 3, A-D). ILI<sup>-</sup> profiles with  
405 no ILI (Fig. 3A), ILI<sup>+1</sup> for profiles displaying a few small ILI 0.1  $\mu$ m in width at most (Fig.  
406 3B), ILI<sup>+2</sup> for profiles displaying several ILI approximately 0.2 to 0.3  $\mu$ m in width (Fig. 3C),  
407 and ILI<sup>+3</sup> for profiles displaying several ILI approximately 0.4 to 0.5  $\mu$ m in width and  
408 occupying most of the mycobacterial cytoplasm (Fig. 3D). The relative abundance of each  
409 type of ILI profile was scored on approximately 200 different mycobacterial profiles per  
410 sample (Fig. 3E). As expected, in the absence of exposure to VLDL, 95% of the *M. bovis*  
411 BCG profiles were ILI<sup>(+1/-)</sup>, regardless of the strain (data not shown). In contrast, after a 24  
412 h exposure to VLDL, ILI<sup>+2</sup> and ILI<sup>+3</sup> were predominantly present among the different *M.*  
413 *bovis* BCG strains (Fig. 3E) as already found with *M. avium* (7). Further examination of

414 the quantitative data showed that both the WT and the LipY-overexpressing strain  
415 displayed similar amounts of ILI profiles of each category with ILI<sup>+3</sup>: 27% ± 4.8 and 25%  
416 ± 4.1; ILI<sup>+2</sup>: 43% ± 3 and 40% ± 4.1; ILI<sup>(+1/-)</sup>: 29% ± 3.9 and 35% ± 6.8, respectively.  
417 Likewise, and as expected, the relative abundance of the 4 types of ILI profiles in the  
418 strain over-expressing the catalytically-inactive form LipY( $\Delta$ PE)<sup>S309A</sup> was similar to the  
419 ones scored in the WT strain and the strain overexpressing LipY (Fig. 3E). In sharp  
420 contrast with these strains, overexpression of LipY( $\Delta$ PE) resulted in a substantial drop in  
421 the percentage of ILI<sup>+3</sup> (15% ± 4.4 vs. 27% ± 4.8) and a concomitant increase in ILI<sup>(+1/-)</sup>  
422 profiles (50% ± 7.5 vs. 29% ± 3.9), as compared to the WT strain. Determination of the  
423 ILI<sup>3+</sup>/ILI<sup>+1/-</sup> ratio profiles showed that overexpression of LipY( $\Delta$ PE) triggers important  
424 changes in the intracellular pool of ILI in comparison with the full-length LipY or the  
425 inactive form LipY( $\Delta$ PE)<sup>S309A</sup> (Fig. 3E). These data are fully consistent with the increased  
426 *in vitro* activity of rLipY( $\Delta$ PE) over rLipY (Table 1).

427

428 **Additional mycobacterial lipases contribute to host TAG hydrolysis and ILI**  
429 **formation.** Despite the primary role of LipY in host lipid hydrolysis, it is very likely that  
430 additional mycobacterial lipases participate in this process, a hypothesis emphasized by  
431 the fact that the genome of *M. tuberculosis* encodes for at least 24 putative lipases (19,  
432 20, 23, 32, 52). To test this hypothesis, macrophages were infected with a *lipY*-deleted  
433 *M. bovis* BCG mutant before being exposed to VLDL for 24 h. The cells were then fixed  
434 and processed for EM and profiles of intracellular mycobacteria were examined for the  
435 presence and extent of ILI formation in both the WT and mutant strains. The profiles of  
436 the mutant clearly displayed smaller ILI than those of the WT strain (Fig. 4A vs 4C). The  
437 relative abundance of each category of ILI was then scored on approximately 150  
438 different mycobacterial profiles per sample (Fig. 4E). Although all categories of ILI were

439 found in the profiles of the  $\Delta lipY$  mutant, the percentage of ILI<sup>3+</sup> profiles was reduced by  
440 approximately 50% (16%  $\pm$  5.8 vs. 35%  $\pm$  2.9) with a concomitant increase in the  
441 percentage of ILI<sup>1/-</sup> (46%  $\pm$  10.9 vs. 27%  $\pm$  5.5) with respect to the WT strain. Functional  
442 complementation of the  $\Delta lipY$  mutant was performed with pMV261::*lipY*, which allows  
443 constitutive expression of the full-length *lipY* leading to the strain  $\Delta lipY::Comp$ . Production  
444 of the protein was confirmed by immunoblotting using polyclonal antibody directed  
445 against the *M. tuberculosis* LipY protein (Fig. 4D). As mentioned earlier (18, 22), LipY is  
446 not produced by wild-type *M. bovis* BCG *in vitro* under standard growth conditions  
447 explaining the lack of a reactive band in the corresponding crude lysate. In contrast, a  
448 specific immunoreactive band was detected in  $\Delta lipY::Comp$ , indicating that LipY is  
449 constitutively produced in this strain. Thus,  $\Delta lipY::Comp$  was used to infect macrophages  
450 for six days, before being exposed to VLDL for 24 h. Analysis of the ILI profile indicates  
451 that complementation restores the WT phenotype, characterized by 39%  $\pm$  5.3 and 23%  
452  $\pm$  4.2 for ILI<sup>3+</sup> and ILI<sup>1/-</sup>, respectively (Fig. 4B and 4E). Likewise, the ILI<sup>3+</sup>/ILI<sup>1/-</sup> ratio was  
453 severely impacted in  $\Delta lipY$  and was restored upon functional complementation of the  
454 mutant, clearly confirming the impact of the *lipY* deletion on intrabacterial lipid  
455 accumulation (Fig 4F).

456 Taken collectively, these results reveal the major contribution of LipY in the  
457 breakdown of host-derived TAG within the phagosomal lumen and highlight the role of  
458 additional mycobacterial lipases in hydrolysis of host TAG and accumulation of TAG in  
459 the form of large ILI.

460  
461 **Consumption of TAG within ILI correlates with the reduction of LB and the activity**  
462 **of cytosolic mycobacterial lipases.** To dissect the physiological link between LB in FM  
463 and ILI in mycobacteria, we had previously investigated whether the formation of large

464 ILI (ILI<sup>+3</sup>) could be reversed by removal of VLDL (7). After exposure of infected  
465 macrophages to VLDL for 24 h, the infected cells had been washed and re-incubated in  
466 fresh medium without lipoprotein. Within 24 h after removal of VLDL, infected cells had  
467 lost their LB and ILI<sup>+3</sup> were no longer visible in the mycobacterial profiles (7), thus  
468 demonstrating the direct link between the presence/absence of LB and ILI  
469 formation/consumption. The same method applied to *M. bovis* BCG-infected cells and the  
470 present work yielded comparable results (Fig. 5D).

471 To determine whether mycobacterial lipases were involved in ILI consumption, we  
472 applied the same chase strategy, but in the absence or presence of lipase inhibitors. After  
473 exposure of WT *M. bovis* BCG-infected cells to VLDL for 24 h to allow ILI formation, the  
474 cells were washed and re-incubated in fresh medium without lipoprotein but in the  
475 absence or presence of either THL or MmPPOX for an additional 24 h. The morphological  
476 appearance of the *M. bovis* BCG profiles was observed under the EM (Fig 5). In the  
477 absence of a lipase inhibitor, ILI<sup>+3</sup> profiles were seldom encountered (Fig. 5A). In contrast,  
478 many ILI<sup>+3</sup> profiles were encountered during a chase in presence of either THL (Fig. 5B)  
479 or MmPPOX (Fig. 5C). Scoring of the relative amount of each category of ILI profiles in  
480 each condition showed, as before (7), that the percentage of ILI<sup>+3</sup> profiles was reduced  
481 by 90% when cells were chased in medium without inhibitors (Fig. 5D). In contrast, when  
482 the chase medium contained either THL or MmPPOX approximately 80 to 90% of the  
483 ILI<sup>+3</sup> profiles were retained (Fig. 5D). The fact that at 24 h the relative abundance of ILI<sup>+3</sup>  
484 was 5 times higher in the presence of THL or MmPPOx (21% ± 0.6 and 23% ± 0.8,  
485 respectively) than in the absence of lipase inhibitors (3.6% ± 0.8) indicates that ILI  
486 consumption is indeed dependent on mycobacterial lipase activity. These results are in  
487 agreement with previous studies showing that hydrolysis of mycobacterial ILI is

488 associated with the decrease of LB in the host (7) and the presence of a (several)  
489 mycobacterial lipase(s) (13, 32), and more particularly LipY (11, 21, 22).

490

## 491 **DISCUSSION**

492 In previous work, VLDL was used as a source of lipids to generate FM (7) since it is  
493 well known that such cells play a major role in the persistence and reactivation phases of  
494 TB within granulomas (5, 6, 11, 53). Quantitative analyses of detailed EM observations  
495 performed after exposure of *M. avium*-infected cells to VLDL had shown that  
496 macrophages became foamy and mycobacteria formed large ILI for which host TAG was  
497 essential. Lipid transfer occurred *via* mycobacterium-induced fusion between LB and  
498 phagosomes. This experimental tool clearly constitutes a well-defined cellular system in  
499 which to study changed metabolic states of intracellular mycobacteria that may relate to  
500 persistence and reactivation of TB. As a follow-up to this proof of concept, this FM model  
501 was used here to demonstrate the extensive accumulation of ILI inside *M. bovis* BCG and  
502 to investigate in detail the role of host lipases in LB formation, without which there can be  
503 no transfer of host TAG to mycobacterium-containing phagosomes, as well as the  
504 physiological role of the mycobacterial lipase, LipY, in the degradation of TAG inside  
505 mycobacterium-containing phagosomes and mycobacterial ILI. By a variety of  
506 approaches, we analyzed the contribution of macrophage and bacterial lipases in LB and  
507 ILI formation/degradation, and propose the following model depicted in **Fig. 6**.

508 After its internalization by receptor-mediated endocytosis, VLDL is transferred to  
509 lysosomes where host lysosomal lipases hydrolyze TAG into its derivatives and free fatty  
510 acid that serves to form LB. In a first set of experiments, we used two different families of  
511 lipase inhibitors, THL and MmPPOX, which, surprisingly, act by targeting different types  
512 of lipases within cells. On the one hand, by exposing infected cells to VLDL in the  
513 presence of THL, this lipase inhibitor shows preferences for host lipases, since TAG  
514 hydrolysis in lysosomes was blocked. Macrophages were unable to become foamy and,  
515 as a result, *M. bovis* BCG was unable to form ILI. On the other hand, exposure of cells to

516 VLDL in presence of *Mm*PPOX, blocked weakly the host lipases in the lysosomes and  
517 consequently did not profoundly affect the formation of LB, but mycobacteria still  
518 remained unable to form ILI. Our results suggest that the effect of this inhibitor is more  
519 specifically directed against mycobacterial lipases. The fact that these two families of  
520 inhibitors target lipases located at different sites could be directly related to their chemical  
521 structures and biophysical properties. In contrast to *Mm*PPOX, THL is indeed a highly  
522 lipophilic molecule with physico-chemical properties similar to those of a diacylglycerol  
523 molecule which makes it soluble in VLDL. By using these two different families of lipase  
524 inhibitors, we can study either the host lipases or the mycobacterial lipases. We,  
525 therefore, provide strong evidence that ILI formation *i*) involves both host lysosomal and  
526 mycobacterial lipases, and *ii*) is strictly dependent on host LB in our experimental model.  
527 In *Dictyostelium discoideum*, *Mycobacterium marinum*, was found to produce ILI without  
528 using TAG as the major carbon source (54, 55). Indeed, the use of a *Dictyostelium*  
529 knockout mutant for both Dgat enzymes (*dgat1* and *dgat2* genes), which is unable to  
530 produce LB, allowed the authors to demonstrate that a resulting excess of free fatty acids  
531 is predominantly incorporated into phospholipids triggering a massive ER-membrane  
532 proliferation. Fluorescent and EM approaches coupled with TLC lipid analyses suggested  
533 that *M. marinum* uses phospholipids to build-up ILI. This observation leads to a new  
534 hypothesis that intracellular mycobacteria have access to a wide range of host lipids, and  
535 one cannot exclude the possibility that bacteria in FM may have direct access to free fatty  
536 acids under conditions other than the experimental conditions of our FM model. Although  
537 this hypothesis has to be fully addressed experimentally in future studies, the current  
538 knowledge about ILI formation in mycobacteria within FM seems to predominantly rely on  
539 host-TAG degradation.

540        Among the large number of lipolytic enzymes encoded by the *M. tuberculosis*  
541 genome, LipY remains the only one carrying an N-terminal PE domain, which was  
542 subsequently found to be a signal of recognition by the ESX-5 secretion system (18, 26).  
543 Herein, we investigated whether the PE domain may directly participate in the enzyme's  
544 TAG activity. Our results are in agreement with a previous study demonstrating that LipY  
545 is the enzyme with the highest potential for hydrolyzing TAG stored inside *M. tuberculosis*  
546 (21). The authors extend our earlier report suggesting that the PE domain plays a role in  
547 modulating the catalytic activity of LipY (22). Comparison of the catalytic activities of rLipY  
548 and rLipY( $\Delta$ PE) clearly indicates that LipY( $\Delta$ PE) is more active than LipY, regardless of  
549 the substrate used. Similar results came from another group who used only one synthetic  
550 non physiological substrate (28). Our data, therefore, add new insights into the functional  
551 role of the PE domain, which is shared by a large number of proteins in pathogenic  
552 mycobacteria. Interestingly, *Mycobacterium marinum* contains a protein homologous to  
553 LipY, termed LipY<sub>mar</sub>, in which the PE domain is substituted by a PPE domain (22). As for  
554 LipY, overexpression of LipY<sub>mar</sub> in *M. smegmatis* significantly reduced the TAG pool, and  
555 this was further pronounced when the PPE domain of LipY<sub>mar</sub> was removed, suggesting  
556 that PE and PPE domains can share a similar functional role. Therefore, given the  
557 analogy between LipY and LipY<sub>mar</sub>, it is conceivable to speculate that the PPE domain,  
558 like the PE domain, directly modulates the activity of LipY<sub>mar</sub> and that the lower catalytic  
559 activity of LipY<sub>mar</sub> may result from steric hindrance of the PPE domain, altering the  
560 recognition/accommodation of TAG within the lipid-binding site. Since, like *M.*  
561 *tuberculosis* or *M. bovis* BCG, *M. marinum* also produces ILI during infection (54) (and  
562 unpublished data), it is tempting to speculate that LipY<sub>mar</sub> plays a crucial role in ILI  
563 formation during *M. marinum* infection.

564 To further delineate the role of the PE domain in modulating the activity of LipY in  
565 an infectious context, experiments were carried out by extending our original  
566 experimental model of FM (7). BMDM were infected with *M. bovis* BCG strains  
567 overexpressing either LipY or LipY( $\Delta$ PE) and exposed to VLDL as a lipid source.  
568 Quantitative analyses of EM observations allowed to perform a detailed investigation on  
569 the role of the mycobacterial lipase, LipY, in the degradation of host TAG transferred to  
570 the mycobacterium-containing phagosomes. Importantly, the difference in *in vitro* activity  
571 of LipY and LipY( $\Delta$ PE) could be reconciled in this model of infection where a significant  
572 reduction of the ILI<sup>+3</sup> category was found with the BCG strain overexpressing LipY( $\Delta$ PE).  
573 This is consistent with the fact that, in contrast to LipY which is secreted, LipY( $\Delta$ PE) fails  
574 to be transported by ESX-5 and, as a consequence, its accumulation inside mycobacteria  
575 boosts ILI degradation (22, 25).

576 In a previous study (7), we had shown that removal of VLDL, induced a rapid  
577 decline of both LB and ILI. Here, we show that exposure of infected cells to lipase  
578 inhibitors, added during the chase period following an exposure to VLDL, strongly affects  
579 TAG hydrolysis within ILI, which remain abundant and large. These results provide  
580 evidence that cytosolic LipY is also involved in ILI consumption.

581 Our data also indicate that the dual localization of LipY impacts on its activity. Since  
582 the PE-containing domain is cleaved off by the ESX-5 secretion system (18), our results  
583 suggest that the mycobacterial surface-anchored form of LipY is more active than the  
584 intracytosolic full-length protein. From these results, it can be inferred that LipY is more  
585 active against host lipids targeted to phagosomes *via* LB-phagosome fusion than towards  
586 TAG stored within ILI. Indeed, as illustrated in (Fig. 6), while a fraction of LipY is found in  
587 the cytosol, consistent with its role in the catabolism of intracellular TAG in ILI, a  
588 significant fraction of mature LipY lacking its PE domain is also localized at the outer

589 surface of the mycobacterial cell envelope, where it catalyzes the breakdown of  
590 exogenously available TAG, such as those found within the LB of the FM. This scenario  
591 is consistent with the idea that *M. tuberculosis* depends on fatty acids as a preferred  
592 energy source during infection (56) where LipY represents a critical enzyme for the  
593 utilization of host lipids. However, the ILI<sup>+3</sup> profile in the mutant  $\Delta lipY$ , clearly indicates the  
594 active participation of other mycobacterial lipases in this process, a finding consistent with  
595 the presence of a large array of lipolytic-encoding genes found in pathogenic  
596 mycobacteria (57). Among these, Rv0183 has been shown to exhibit a preference for  
597 MAG or DAG and to be localized to the cell wall (19, 58), whereas Cfp21, a secreted  
598 cutinase-like enzyme also expresses TAG lipase activity (20, 52). These two proteins may  
599 represent putative candidates which, in addition to LipY, may participate in the breakdown  
600 of host TAG transferred to phagosomes, and the release of free fatty acids which may be  
601 utilized by multiple TAG synthases (59) to carry out the synthesis of TAG in the  
602 mycobacterial cytosol (Fig. 6). Utilization of these TAG in ILI is essential for the regrowth  
603 of mycobacteria during their exit from hypoxic non-replicating conditions (32) and  
604 reactivation of latent infection to cause an active disease.

605

## 606 **ACKNOWLEDGMENTS**

607 We are grateful to S. Rao (Novartis Institute for Tropical Diseases, Singapore) for  
608 the kind gift of the *lipY* deletion mutant. PS received financial support for his PhD  
609 fellowship from the Ministère Français de l'Enseignement Supérieur, de la Recherche et  
610 de l'Innovation. The authors wish to thank the support by the Fondation pour la Recherche  
611 Médicale (FRM) (DEQ20150331719) to LK and Campus France (Paris, France) for the  
612 PhD fellowship granted to SD. This work was supported by core grants from the Institut  
613 National de la Santé et de la Recherche Médicale (Inserm) and the Centre National de la  
614 Recherche Scientifique (CNRS), and by grant number ANR-09-MIEN-009-03 from the  
615 Agence Nationale de la Recherche (French National Research Agency) to LA., CdC., LK.  
616 and SC. The EM observations and analyses were performed by CdC and IP in the PiCSL  
617 EM core facility (Institut de Biologie du Développement, Aix-Marseille Université,  
618 Marseille), a member of the France-BioImaging French research infrastructure. This work  
619 has also benefited from the facilities and expertise of the Platform for Microscopy of IMM  
620 (Institut de Microbiologie de la Méditerranée).

621 The authors wish to thank the members of these EM facilities for expert technical  
622 assistance, Jean Pierre Gorvel (Centre d'Immunologie de Marseille-Luminy, Aix-Marseille  
623 Université UM2, Inserm, U1104, CNRS UMR7280, Marseille, 13288, France) for  
624 continuous support and advice, Irène Caire-Brändli for expert technical assistance, she  
625 took part in the cellular microbiology experiments and EM observations and analyses  
626 under CdC's supervision. We would like to thank Pr Valéry Matarazzo and members from  
627 the INMED laboratory (INSERM-INMED UMR901, Aix-Marseille Université) for providing  
628 the femurs of 6- to 8-week-old C57BL/6 female mice. Finally, we kindly thank and Jean-  
629 François Cavalier (CNRS, UMR7255, Marseille, France) for providing the *MmPPOX*  
630 lipase inhibitor and for fruitful discussions.

631 **FIGURE LEGENDS**

632 **Figure 1: Addition of lipase inhibitors during exposure to VLDL affects host LB**  
633 **formation and accumulation of mycobacterial lipids in the form of ILI.** At day 6 p.i.  
634 with WT *M. bovis* BCG, BMDM were exposed for 24 h to VLDL in the absence or presence  
635 of lipase inhibitors. The cells were then processed for EM and analyzed for host LB and  
636 mycobacterial ILI formation. **(A, B, E)** Morphological appearance of host LB and  
637 lysosomes (Ly): **(A)** exposure to VLDL and THL: LB are scarce and Ly are filled with  
638 electron-translucent lipids (Ly<sup>+</sup>); **(B)** exposure to VLDL only: cells contain many LB and  
639 Ly retain their normal appearance, with dense contents only; **(E)** exposure to VLDL and  
640 *MmPPOX*: LB are present and most Ly either retain their normal appearance or contain  
641 low amounts of lipids in the form of lipid droplets (Ly<sup>+/-</sup>). **(C, D, F)** Morphological  
642 appearance of ILI within mycobacterial profiles: **(C)** exposure to VLDL and THL: no ILI<sup>+3</sup>  
643 mycobacterial profiles; **(D)** Exposure to VLDL only: many mycobacterial profiles are ILI<sup>+3</sup>;  
644 **(F)** Exposure to VLDL and *MmPPOX*: ILI remained small and no ILI<sup>+3</sup> mycobacterial  
645 profiles were observed. Bars in panels **A to F**, 0.5  $\mu\text{m}$ . **(G)** Dependence of steady-state  
646 levels of ILI<sup>+3</sup>, ILI<sup>+2</sup> and ILI<sup>+1/-</sup> profiles on the absence or presence of lipase inhibitors. Error  
647 bars indicate the standard deviations (SD) based on the results of 2 to 4 independent  
648 experiments. For each experiment, 150 to 300 profiles were examined for each treatment.  
649 Statistical analysis was performed by using two tailed Student's *t*-test. Results were  
650 compared to an untreated sample and \*\* correspond to a *P* value <0.01 and \*\*\*  
651 correspond to a *P* value <0.001.

652

653 **Figure 2: Purification and structural modelling of LipY and LipY( $\Delta$ PE).** **(A)** Protein  
654 purity assessed on SDS-PAGE. Six  $\mu\text{g}$  of protein were loaded onto a 12% polyacrylamide

655 gel and stained with Instant Blue solution. Lane 1, rLipY; lane 2, rLipY( $\Delta$ PE). MW,  
656 Molecular Weight standards (10  $\mu$ g, Euromedex). **(B)** Alignment of the LipY and  
657 LipY( $\Delta$ PE) amino acid sequences. The secondary structures identified from the  
658 corresponding three-dimensional models are indicated above the sequences using the  
659 same color codes as those used in the structural models depicted in C: PE domain in  
660 blue, linker unit in green and catalytic domain in pink. Black stars below the sequence  
661 indicate the catalytic triad. **(C)** Overall view of the structural models of LipY and  
662 LipY( $\Delta$ PE). On the left part, the LipY and LipY( $\Delta$ PE) 3D-models were generated by I-  
663 TASSER software. The PE domain is represented in blue and in both cases, the catalytic  
664 triad composed of serine (Ser309), aspartic acid (Asp383) and histidine (His414) residues  
665 are also indicated. The green part represents the polypeptide linking the catalytic domain  
666 to the PE domain. The black arrow shows the displacement of the linker after deletion of  
667 the PE domain, leading to a large opening of the active site and allowing a better  
668 accommodation of the substrates.

669 **Figure 3: Distribution of ILI profiles in *M. bovis* BCG strains over-expressing**  
670 **various LipY variants in VLDL-driven FM.** BMDM were infected with BCG strains over-  
671 expressing different LipY variants. After exposure to VLDL for 24 h, cells were fixed, and  
672 processed for EM. Bacterial profiles were divided into 4 different categories in terms of  
673 the presence and size of ILI (ILI<sup>-</sup>, ILI<sup>+1</sup>, ILI<sup>+2</sup>, ILI<sup>+3</sup>). **(A)** ILI<sup>-</sup> is no ILI. **(B)** ILI<sup>+1</sup> is less than 5  
674 small ILI up to 0.1  $\mu$ m in width. **(C)** ILI<sup>+2</sup> is several ILI 0.2 to 0.3  $\mu$ m in width. **(D)** ILI<sup>+3</sup> is  
675 several ILI 0.4 to 0.5  $\mu$ m in width and extending across the full width of the *M. bovis* BCG  
676 cytosol. Bars in panels A to D, 0.5  $\mu$ m. **(E)** Comparative analysis of the percentage of  
677 each category of ILI profiles in wild-type (WT) vs. *M. bovis* BCG strains over-expressing  
678 different LipY variants (LipY, LipY( $\Delta$ PE), LipY( $\Delta$ PE)<sup>S309A</sup>). Error bars indicate the standard  
679 deviations based on the results of 2 to 4 independent experiments. For each experiment,

680 100 to 250 profiles were examined for each strain. Statistical analysis was performed by  
681 using two tailed Student's *t*-test. Results were compared to the WT strain and \*  
682 correspond to a *P* value <0.05 and \*\* correspond to a *P* value <0.01. **(F)** Comparative  
683 analysis of ILI<sup>3+</sup>/ILI<sup>1+/-</sup> ratios in WT and LipY overexpressing strains. Ratios were  
684 calculated by dividing the percentage of ILI<sup>3+</sup> with the percentage of ILI<sup>1+/-</sup> bacteria  
685 collected between 2 to 4 independent experiments. Error bars indicate the standard  
686 deviations and statistical analysis was performed by using two tailed Student's *t*-test  
687 where \* correspond to a *P* value <0.05 and \*\* correspond to a *P* value <0.01.

688 **Figure 4: LipY and additional mycobacterial lipases contribute to host TAG**  
689 **hydrolysis and ILI formation.** At day 6 p.i. with either WT *M. bovis* BCG,  $\Delta lipY$  or  $\Delta lipY$   
690 complemented ( $\Delta lipY::Comp$ ) strains, BMDM were exposed for 24 h to VLDL. The cells  
691 were then processed for EM and analysed for mycobacterial ILI formation. **(A)** BMDM  
692 infected with the  $\Delta lipY$  strain: most of the ILI profiles were small, **(B)** BMDM infected with  
693 the  $\Delta lipY::Comp$  strain: numerous large ILI were observed, **(C)** BMDM infected with WT  
694 *M. bovis* BCG: ILI<sup>+3</sup> profiles were abundant. Bars in panels A and C, 0.5  $\mu$ m and B 1  $\mu$ m,  
695 **(D)** Western blot analysis of WT,  $\Delta lipY$  or  $\Delta lipY::Comp$  strains. Equal amounts of lysates  
696 were immunoblotted and the full-length LipY was detected using a polyclonal antibody.  
697 GroEL2 was included as a loading control. **(E)** Comparative evaluation of the percentage  
698 of each category of ILI profiles formed in either the WT or the  $\Delta lipY$  strain. Error bars  
699 indicate the standard deviations based on the results of 2 to 4 independent experiments.  
700 For each experiment, 150 to 300 profiles were examined for each treatment. Statistical  
701 analysis was performed with the two-tailed Student's *t*-test. Results were compared to  
702 the WT strain and \* correspond to a *P* value <0.05. **(F)** Comparative analysis of ILI<sup>3+</sup>/ILI<sup>1+/-</sup>  
703 ratio of WT,  $\Delta lipY$  or  $\Delta lipY::Comp$  strains. Ratios were calculated by dividing the  
704 percentage of ILI<sup>3+</sup> with the percentage of ILI<sup>1+/-</sup> bacteria collected between 2 to 4

705 independent experiments. Error bars indicate the standard deviations (SD) and statistical  
706 analysis was performed with the two tailed Student's *t*-test where \* correspond to a *P*  
707 value <0.05.

708

709 **Figure 5: Consumption of TAG within ILI correlates with the activity of cytosolic**  
710 **mycobacterial lipases.** At day 6 p.i. with WT *M. bovis* BCG, BMDM were exposed to  
711 VLDL for 24 h and then re-incubated in VLDL-free culture medium without or with THL or  
712 *MmPPOX* for 24 h. The cells were then processed for EM and the percentage of each  
713 category of ILI profiles was assessed. **(A)** VLDL for 24 h followed by a 24 h-chase in  
714 medium devoid of inhibitors. Cells contain few ILI<sup>+3</sup> profiles. **(B)** VLDL for 24 h followed  
715 by a 24 h-chase in medium with THL. Cells still contain ILI<sup>+3</sup> profiles. **(C)** VLDL for 24 h  
716 followed by a 24 h-chase in medium with *MmPPOX*. Cells still contain ILI<sup>+3</sup> profiles. Bars  
717 in panels A and B, 0.5 μm and C 0.7 μm **(D)** Quantitative evaluation of the percentage of  
718 each category of ILI profiles immediately after a 24 h exposure to VLDL (no I, 0 h) or after  
719 a 24 h chase in culture medium without inhibitor (no I, 24 h), with THL (THL, 24 h) or with  
720 *MmPPOX* (*MmPPOX*, 24 h). Error bars indicate the standard deviations based on the  
721 results of 2 to 3 independent experiments. For each experiment, 150 to 300 profiles were  
722 examined for each treatment. Statistical analysis was performed by using two tailed  
723 Student's *t*-test. Results without inhibitors were compared to the "No I 0h" condition where  
724 # correspond to a *P* value <0.05 and ## correspond to a *P* value <0.01. Whereas results  
725 with the inhibitors were compared to the "No I 24 h" condition where \* correspond to a  
726 *P* value <0.05 and \*\* correspond to a *P* value <0.01

727 **Figure 6: Proposed model for LipY *in vivo* activity as a function of its localization.**  
728 The PE domain of LipY functions as a secretion signal recognized by the ESX-5 secretion

729 system. **(1)**: Endocytic uptake of VLDL composed of phospholipids (P), triglycerides (T)  
730 and cholesterol (C) and transfer to lysosomes (Ly). **(2)**: Hydrolysis of TAG in VLDL and  
731 formation of TAG-rich host LB after release of free fatty acids (FA) from Ly. **(3)**: Fusion of  
732 LB with the membrane of mycobacterium-containing phagosomes. Host TAG is released  
733 into the phagosomal lumen during this process. **(4)**: During its translocation across the  
734 mycobacterial cell envelope *via* ESX-5, the LipY N-terminal PE domain is cleaved off.  
735 After secretion into the phagosome, LipY( $\Delta$ PE) remains closely associated with the  
736 mycobacterial outermost surface, where it hydrolyses host TAG. At this stage, other  
737 mycobacterial lipases are likely to be involved in the degradation of the LipY end-product,  
738 releasing free fatty acid (FA), which are then transported to the mycobacterial cytosol  
739 where TAG are resynthesized by the TAG synthases (TGS). TAG then accumulate to  
740 form intracytosolic lipid inclusions (ILI). **(5)**: Under specific conditions, TAG within ILI can  
741 be hydrolyzed by cytosolic LipY.

742

743 **Table 1:** Specific activities of rLipY and rLipY( $\Delta$ PE) on various lipid substrates<sup>a</sup>.

Substrates	Specific activity (U*/mg)		
	rLipY	rLipY( $\Delta$ PE)	rLipY( $\Delta$ PE)/ rLipY
Monobutyrim <sup>(b)</sup> (MC4)	61.0 $\pm$ 2.0	92.0 $\pm$ 5.0	1.5
Monolein <sup>(a)</sup> (MC18)	6.6 $\pm$ 0.5	17.0 $\pm$ 1.0	2.5
Diolein <sup>(a)</sup> (DC18)	3.5 $\pm$ 0.2	5.6 $\pm$ 0.4	1.6
Tributyrim <sup>(b)</sup> (TC4)	129.0 $\pm$ 6.0	267.0 $\pm$ 24.0	2.0
Trioctanoin <sup>(a)</sup> (TC8)	20.0 $\pm$ 2.0	38.0 $\pm$ 1.0	1.9
Pomegranate oil TAG	4.0 $\pm$ 0.2	4.8 $\pm$ 0.3	1.2

744

745 <sup>a</sup> All substrates were assayed at concentrations above their solubility limits. Experiments  
 746 were performed at 37°C in 15 mL of 2.5 mM Tris-HCl buffer (pH 7.5) containing 300 mM  
 747 NaCl and 1<sup>(a)</sup> or 3<sup>(b)</sup> mM NaTDC. \* One unit corresponds to 1  $\mu$ mole of fatty acid released  
 748 per min. Values are means of 3 independent experiments  $\pm$  SD.

749

750 **References**

751

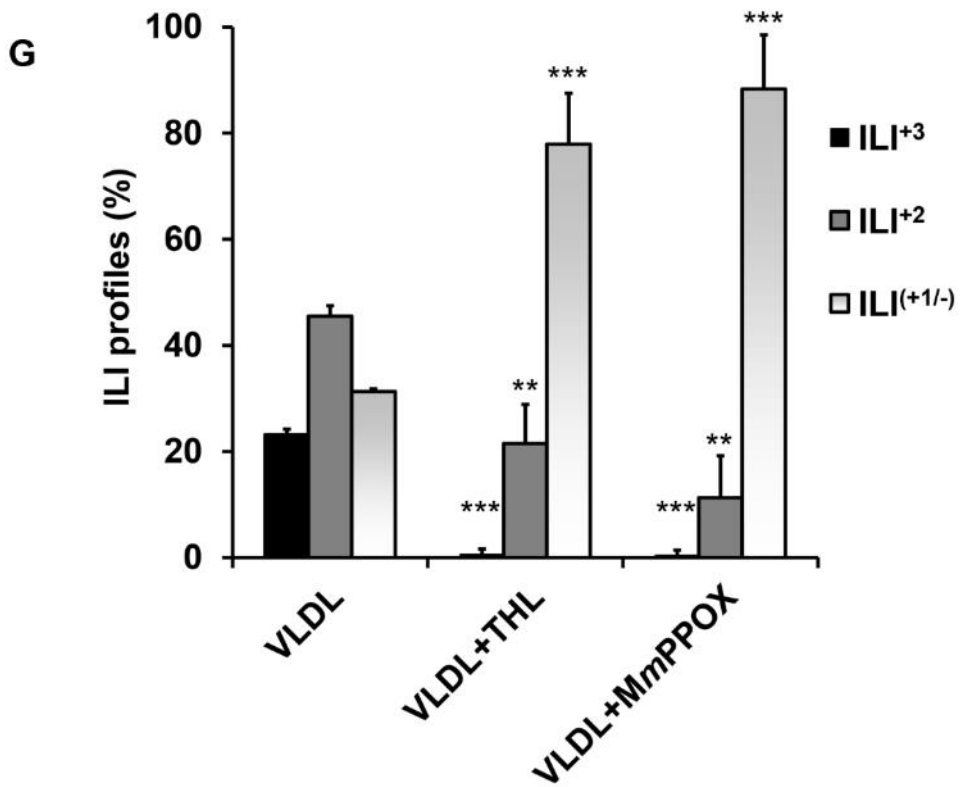
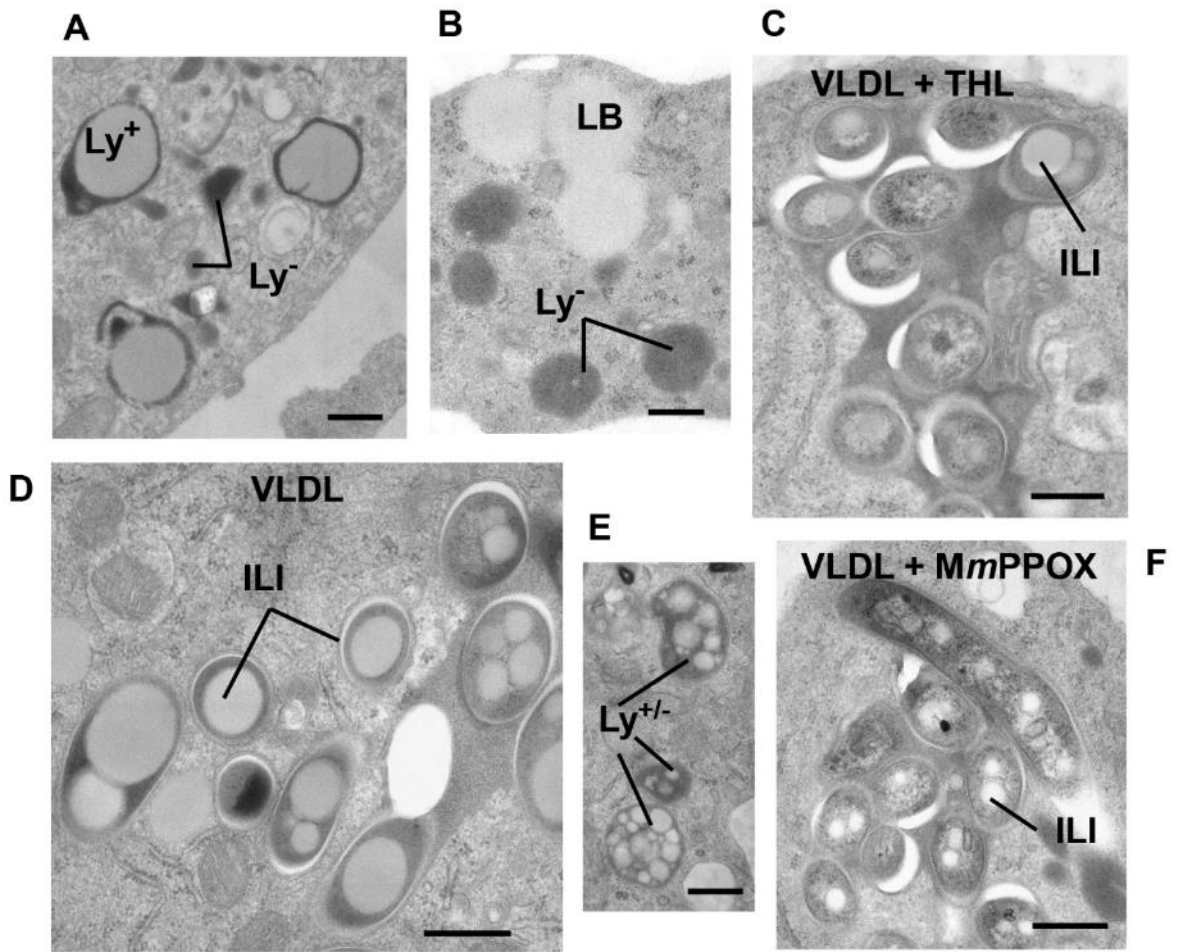
- 752 1. WHO. 2017. Global Tuberculosis Report
- 753 2. Irwin SM, Driver E, Lyon E, Schrupp C, Ryan G, Gonzalez-Juarrero M,  
754 Basaraba RJ, Nuermberger EL, Lenaerts AJ. 2015. Presence of multiple lesion  
755 types with vastly different microenvironments in C3HeB/FeJ mice following  
756 aerosol infection with *Mycobacterium tuberculosis*. *Disease models &*  
757 *mechanisms* 8:591-602.
- 758 3. Lenaerts A, Barry CE, 3rd, Dartois V. 2015. Heterogeneity in tuberculosis  
759 pathology, microenvironments and therapeutic responses. *Immunological*  
760 *reviews* 264:288-307.
- 761 4. Manina G, Dhar N, McKinney JD. 2015. Stress and host immunity amplify  
762 *Mycobacterium tuberculosis* phenotypic heterogeneity and induce nongrowing  
763 metabolically active forms. *Cell host & microbe* 17:32-46.
- 764 5. Peyron P, Vaubourgeix J, Poquet Y, Levillain F, Botanch C, Bardou F, Daffe M,  
765 Emile JF, Marchou B, Cardona PJ, de Chastellier C, Altare F. 2008. Foamy  
766 macrophages from tuberculous patients' granulomas constitute a nutrient-rich  
767 reservoir for *M. tuberculosis* persistence. *PLoS Pathog* 4:e1000204.
- 768 6. Hunter RL, Jagannath C, Actor JK. 2007. Pathology of postprimary tuberculosis  
769 in humans and mice: contradiction of long-held beliefs. *Tuberculosis (Edinb)*  
770 87:267-78.
- 771 7. Caire-Brandli I, Papadopoulos A, Malaga W, Marais D, Canaan S, Thilo L, de  
772 Chastellier C. 2014. Reversible Lipid Accumulation and Associated Division  
773 Arrest of *Mycobacterium avium* in Lipoprotein-Induced Foamy Macrophages  
774 May Resemble Key Events during Latency and Reactivation of Tuberculosis.  
775 *Infection and immunity* 82:476-90.
- 776 8. Garton NJ, Waddell SJ, Sherratt AL, Lee SM, Smith RJ, Senner C, Hinds J,  
777 Rajakumar K, Adegbola RA, Besra GS, Butcher PD, Barer MR. 2008.  
778 Cytological and transcript analyses reveal fat and lazy persister-like bacilli in  
779 tuberculous sputum. *PLoS Med* 5:e75.
- 780 9. Daniel J, Sirakova T, Kolattukudy P. 2014. An acyl-CoA synthetase in  
781 *Mycobacterium tuberculosis* involved in triacylglycerol accumulation during  
782 dormancy. *PLoS ONE* 9:e114877.
- 783 10. Daniel J, Maamar H, Deb C, Sirakova TD, Kolattukudy PE. 2011.  
784 *Mycobacterium tuberculosis* uses host triacylglycerol to accumulate lipid  
785 droplets and acquires a dormancy-like phenotype in lipid-loaded macrophages.  
786 *PLoS Pathog* 7:e1002093.
- 787 11. Kapoor N, Pawar S, Sirakova TD, Deb C, Warren WL, Kolattukudy PE. 2013.  
788 Human granuloma in vitro model, for TB dormancy and resuscitation. *PLoS*  
789 *ONE* 8:e53657.
- 790 12. Viljoen A, Blaise M, de Chastellier C, Kremer L. 2016. MAB\_3551c encodes the  
791 primary triacylglycerol synthase involved in lipid accumulation in *Mycobacterium*  
792 *abscessus*. *Molecular microbiology*.
- 793 13. Dhouib R, Ducret A, Hubert P, Carriere F, Dukan S, Canaan S. 2011. Watching  
794 intracellular lipolysis in mycobacteria using time lapse fluorescence microscopy.  
795 *Biochim Biophys Acta* 1811:234-41.
- 796 14. Santucci P, Bouzid F, Smichi N, Poncin I, Kremer L, De Chastellier C, Drancourt  
797 M, Canaan S. 2016. Experimental Models of Foamy Macrophages and  
798 Approaches for Dissecting the Mechanisms of Lipid Accumulation and

- 799 Consumption during Dormancy and Reactivation of Tuberculosis. *Frontiers in*  
800 *cellular and infection microbiology* 6:122.
- 801 15. Daniel J, Kapoor N, Sirakova T, Sinha R, Kolattukudy P. 2016. The perilipin-like  
802 PPE15 protein in *Mycobacterium tuberculosis* is required for triacylglycerol  
803 accumulation under dormancy-inducing conditions. *Molecular microbiology*.  
804 16. Dedieu L, Serveau-Avesque C, Kremer L, Canaan S. 2013. Mycobacterial  
805 lipolytic enzymes: a gold mine for tuberculosis research. *Biochimie* 95:66-73.  
806 17. Singh G, Jadeja D, Kaur J. 2010. Lipid hydrolyzing enzymes in virulence:  
807 *Mycobacterium tuberculosis* as a model system. *Crit Rev Microbiol* 36:259-69.  
808 18. Daleke MH, Cascioferro A, de Punder K, Ummels R, Abdallah AM, van der Wel  
809 N, Peters PJ, Luirink J, Manganelli R, Bitter W. 2011. Conserved Pro-Glu (PE)  
810 and Pro-Pro-Glu (PPE) protein domains target LipY lipases of pathogenic  
811 mycobacteria to the cell surface via the ESX-5 pathway. *J Biol Chem*  
812 286:19024-34.  
813 19. Dhouib R, Laval F, Carriere F, Daffe M, Canaan S. 2010. A monoacylglycerol  
814 lipase from *Mycobacterium smegmatis* Involved in bacterial cell interaction. *J*  
815 *Bacteriol* 192:4776-85.  
816 20. Schué M, Maurin D, Dhouib R, N'Goma JC, Delorme V, Lambeau G, Carriere  
817 F, Canaan S. 2010. Two cutinase-like proteins secreted by *Mycobacterium*  
818 *tuberculosis* show very different lipolytic activities reflecting their physiological  
819 function. *Faseb J* 24:1893-903.  
820 21. Deb C, Daniel J, Sirakova TD, Abomoelak B, Dubey VS, Kolattukudy PE. 2006.  
821 A novel lipase belonging to the hormone-sensitive lipase family induced under  
822 starvation to utilize stored triacylglycerol in *Mycobacterium tuberculosis*. *J Biol*  
823 *Chem* 281:3866-75.  
824 22. Mishra KC, de Chastellier C, Narayana Y, Bifani P, Brown AK, Besra GS,  
825 Katoch VM, Joshi B, Balaji KN, Kremer L. 2008. Functional role of the PE  
826 domain and immunogenicity of the *Mycobacterium tuberculosis* triacylglycerol  
827 hydrolase LipY. *Infection and immunity* 76:127-40.  
828 23. Delorme V, Diomande SV, Dedieu L, Cavalier JF, Carriere F, Kremer L, Leclair  
829 J, Fotiadu F, Canaan S. 2012. MmPPOX inhibits *Mycobacterium tuberculosis*  
830 lipolytic enzymes belonging to the hormone-sensitive lipase family and alters  
831 mycobacterial growth. *PLoS One* 7:e46493.  
832 24. Abdallah AM, Gey van Pittius NC, Champion PA, Cox J, Luirink J,  
833 Vandenbroucke-Grauls CM, Appelmelk BJ, Bitter W. 2007. Type VII secretion-  
834 -mycobacteria show the way. *Nat Rev Microbiol* 5:883-91.  
835 25. Abdallah AM, Verboom T, Weerdenburg EM, Gey van Pittius NC, Mahasha PW,  
836 Jimenez C, Parra M, Cadieux N, Brennan MJ, Appelmelk BJ, Bitter W. 2009.  
837 PPE and PE\_PGRS proteins of *Mycobacterium marinum* are transported via  
838 the type VII secretion system ESX-5. *Molecular microbiology* 73:329-40.  
839 26. Daleke MH, Ummels R, Bawono P, Heringa J, Vandenbroucke-Grauls CM,  
840 Luirink J, Bitter W. 2012. General secretion signal for the mycobacterial type VII  
841 secretion pathway. *Proceedings of the National Academy of Sciences of the*  
842 *United States of America* 109:11342-7.  
843 27. Chaturvedi R, Bansal K, Narayana Y, Kapoor N, Sukumar N, Togarsimalemath  
844 SK, Chandra N, Mishra S, Ajitkumar P, Joshi B, Katoch VM, Patil SA, Balaji KN.  
845 2010. The multifunctional PE\_PGRS11 protein from *Mycobacterium*  
846 *tuberculosis* plays a role in regulating resistance to oxidative stress. *J Biol Chem*  
847 285:30389-403.

- 848 28. Garrett CK, Broadwell LJ, Hayne CK, Neher SB. 2015. Modulation of the Activity  
849 of *Mycobacterium tuberculosis* LipY by Its PE Domain. *PLoS ONE*  
850 10:e0135447.
- 851 29. Neyrolles O. 2014. Mycobacteria and the greasy macrophage: getting fat and  
852 frustrated. *Infection and immunity* 82:472-5.
- 853 30. Noens EE, Williams C, Anandhakrishnan M, Poulsen C, Ehebauer MT,  
854 Wilmanns M. 2011. Improved mycobacterial protein production using a  
855 *Mycobacterium smegmatis* groEL1DeltaC expression strain. *BMC Biotechnol*  
856 11:27.
- 857 31. Goude R, Roberts DM, Parish T. 2015. Electroporation of mycobacteria.  
858 *Methods Mol Biol* 1285:117-30.
- 859 32. Low KL, Rao PS, Shui G, Bendt AK, Pethe K, Dick T, Wenk MR. 2009.  
860 Triacylglycerol utilization is required for regrowth of in vitro hypoxic  
861 nonreplicating *Mycobacterium bovis* bacillus Calmette-Guerin. *J Bacteriol*  
862 191:5037-43.
- 863 33. Kong TH, Coates AR, Butcher PD, Hickman CJ, Shinnick TM. 1993.  
864 *Mycobacterium tuberculosis* expresses two chaperonin-60 homologs.  
865 *Proceedings of the National Academy of Sciences of the United States of*  
866 *America* 90:2608-12.
- 867 34. Ojha A, Anand M, Bhatt A, Kremer L, Jacobs WR, Jr., Hatfull GF. 2005. GroEL1:  
868 a dedicated chaperone involved in mycolic acid biosynthesis during biofilm  
869 formation in mycobacteria. *Cell* 123:861-73.
- 870 35. Daugelat S, Kowall J, Mattow J, Bumann D, Winter R, Hurwitz R, Kaufmann SH.  
871 2003. The RD1 proteins of *Mycobacterium tuberculosis*: expression in  
872 *Mycobacterium smegmatis* and biochemical characterization. *Microbes Infect*  
873 5:1082-95.
- 874 36. Stover CK, de la Cruz VF, Fuerst TR, Burlein JE, Benson LA, Bennett LT,  
875 Bansal GP, Young JF, Lee MH, Hatfull GF, et al. 1991. New use of BCG for  
876 recombinant vaccines. *Nature* 351:456-60.
- 877 37. Brust B, Lecoufle M, Tuaille E, Dedieu L, Canaan S, Valverde V, Kremer L.  
878 2011. *Mycobacterium tuberculosis* lipolytic enzymes as potential biomarkers for  
879 the diagnosis of active tuberculosis. *PLoS One* 6:e25078.
- 880 38. Laemmli UK. 1970. Cleavage of structural proteins during the assembly of the  
881 head of bacteriophage T4. *Nature* 227:680-685.
- 882 39. Point V, Malla RK, Diomande S, Martin BP, Delorme V, Carriere F, Canaan S,  
883 Rath NP, Spilling CD, Cavalier JF. 2012. Synthesis and kinetic evaluation of  
884 cyclophostin and cyclipostins phosphonate analogs as selective and potent  
885 inhibitors of microbial lipases. *J Med Chem* 55:10204-19.
- 886 40. Ulker S, Placidi C, Point V, Gadenne B, Serveau-Avesque C, Canaan S,  
887 Carriere F, Cavalier JF. 2015. New lipase assay using Pomegranate oil coating  
888 in microtiter plates. *Biochimie*.
- 889 41. Roy A, Kucukural A, Zhang Y. 2010. I-TASSER: a unified platform for  
890 automated protein structure and function prediction. *Nature protocols* 5:725-38.
- 891 42. Zhang Y. 2008. I-TASSER server for protein 3D structure prediction. *BMC*  
892 *Bioinformatics* 9:40.
- 893 43. Corpet F. 1988. Multiple sequence alignment with hierarchical clustering.  
894 *Nucleic Acids Research* 16:10881-90.
- 895 44. Robert X, Gouet P. 2014. Deciphering key features in protein structures with the  
896 new ENDscript server. *Nucleic Acids Research* 42:W320-4.

- 897 45. Hadvary P, Lengsfeld H, Wolfer H. 1988. Inhibition of pancreatic lipase *in vitro*  
898 by the covalent inhibitor tetrahydrolipstatin. *Biochemical Journal* 256:357-361.
- 899 46. Yang PY, Liu K, Ngai MH, Lear MJ, Wenk MR, Yao SQ. 2010. Activity-based  
900 proteome profiling of potential cellular targets of Orlistat--an FDA-approved drug  
901 with anti-tumor activities. *J Am Chem Soc* 132:656-66.
- 902 47. Nelson RH, Miles JM. 2005. The use of orlistat in the treatment of obesity,  
903 dyslipidaemia and Type 2 diabetes. *Expert Opin Pharmacother* 6:2483-91.
- 904 48. Hadvary P, Sidler W, Meister W, Vetter W, Wolfer H. 1991. The lipase inhibitor  
905 tetrahydrolipstatin binds covalently to the putative active site serine of  
906 pancreatic lipase. *J Biol Chem* 266:2021-2027.
- 907 49. Ravindran MS, Rao SP, Cheng X, Shukla A, Cazenave-Gassiot A, Yao SQ,  
908 Wenk MR. 2014. Targeting Lipid Esterases in Mycobacteria Grown Under  
909 Different Physiological Conditions Using Activity-based Profiling with  
910 Tetrahydrolipstatin (THL). *Molecular & cellular proteomics : MCP* 13:435-48.
- 911 50. Ben Ali Y, Chahinian H, Petry S, Muller G, Lebrun R, Verger R, Carriere F,  
912 Mandrich L, Rossi M, Manco G, Sarda L, Abousalham A. 2006. Use of an  
913 inhibitor to identify members of the hormone-sensitive lipase family.  
914 *Biochemistry* 45:14183-91.
- 915 51. Fishbein S, van Wyk N, Warren RM, Sampson SL. 2015. Phylogeny to function:  
916 PE/PPE protein evolution and impact on Mycobacterium tuberculosis  
917 pathogenicity. *Molecular microbiology* 96:901-16.
- 918 52. West NP, Chow FM, Randall EJ, Wu J, Chen J, Ribeiro JM, Britton WJ. 2009.  
919 Cutinase-like proteins of Mycobacterium tuberculosis: characterization of their  
920 variable enzymatic functions and active site identification. *FASEB J* 23:1694-  
921 704.
- 922 53. Russell DG, Cardona PJ, Kim MJ, Allain S, Altare F. 2009. Foamy macrophages  
923 and the progression of the human tuberculosis granuloma. *Nat Immunol* 10:943-  
924 8.
- 925 54. Barisch C, Paschke P, Hagedorn M, Maniak M, Soldati T. 2015. Lipid droplet  
926 dynamics at early stages of Mycobacterium marinum infection in Dictyostelium.  
927 *Cellular microbiology*.
- 928 55. Barisch C, Soldati T. 2017. Mycobacterium marinum Degrades Both  
929 Triacylglycerols and Phospholipids from Its Dictyostelium Host to Synthesise Its  
930 Own Triacylglycerols and Generate Lipid Inclusions. *PLoS pathogens*  
931 13:e1006095.
- 932 56. Munoz-Elias EJ, McKinney JD. 2006. Carbon metabolism of intracellular  
933 bacteria. *Cellular microbiology* 8:10-22.
- 934 57. Cole ST, Brosch R, Parkhill J, Garnier T, Churcher C, Harris D, Gordon SV,  
935 Eiglmeier K, Gas S, Barry CE, 3rd, Tekaia F, Badcock K, Basham D, Brown D,  
936 Chillingworth T, Connor R, Davies R, Devlin K, Feltwell T, Gentles S, Hamlin N,  
937 Holroyd S, Hornsby T, Jagels K, Barrell BG, et al. 1998. Deciphering the biology  
938 of *Mycobacterium tuberculosis* from the complete genome sequence. *Nature*  
939 393:537-44.
- 940 58. Cotes K, Dhouib R, Douchet I, Chahinian H, de Caro A, Carriere F, Canaan S.  
941 2007. Characterization of an exported monoglyceride lipase from  
942 Mycobacterium tuberculosis possibly involved in the metabolism of host cell  
943 membrane lipids. *Biochem J* 408:417-27.
- 944 59. Daniel J, Deb C, Dubey VS, Sirakova TD, Abomoelak B, Morbidoni HR,  
945 Kolattukudy PE. 2004. Induction of a novel class of diacylglycerol  
946 acyltransferases and triacylglycerol accumulation in *Mycobacterium*

947           *tuberculosis* as it goes into a dormancy-like state in culture. J Bacteriol  
948           186:5017-30.  
949  
950  
  
951



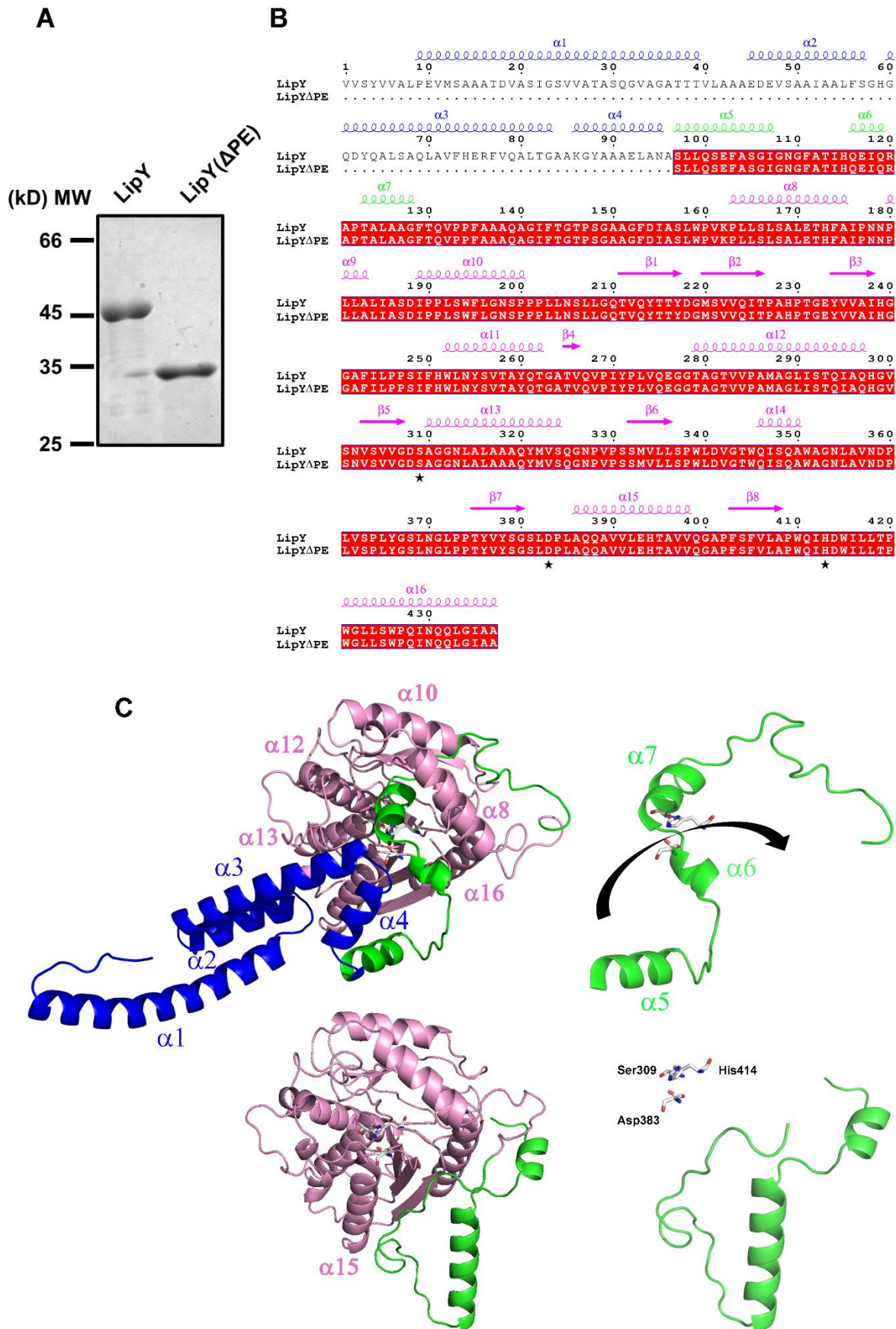


**Figure 3**

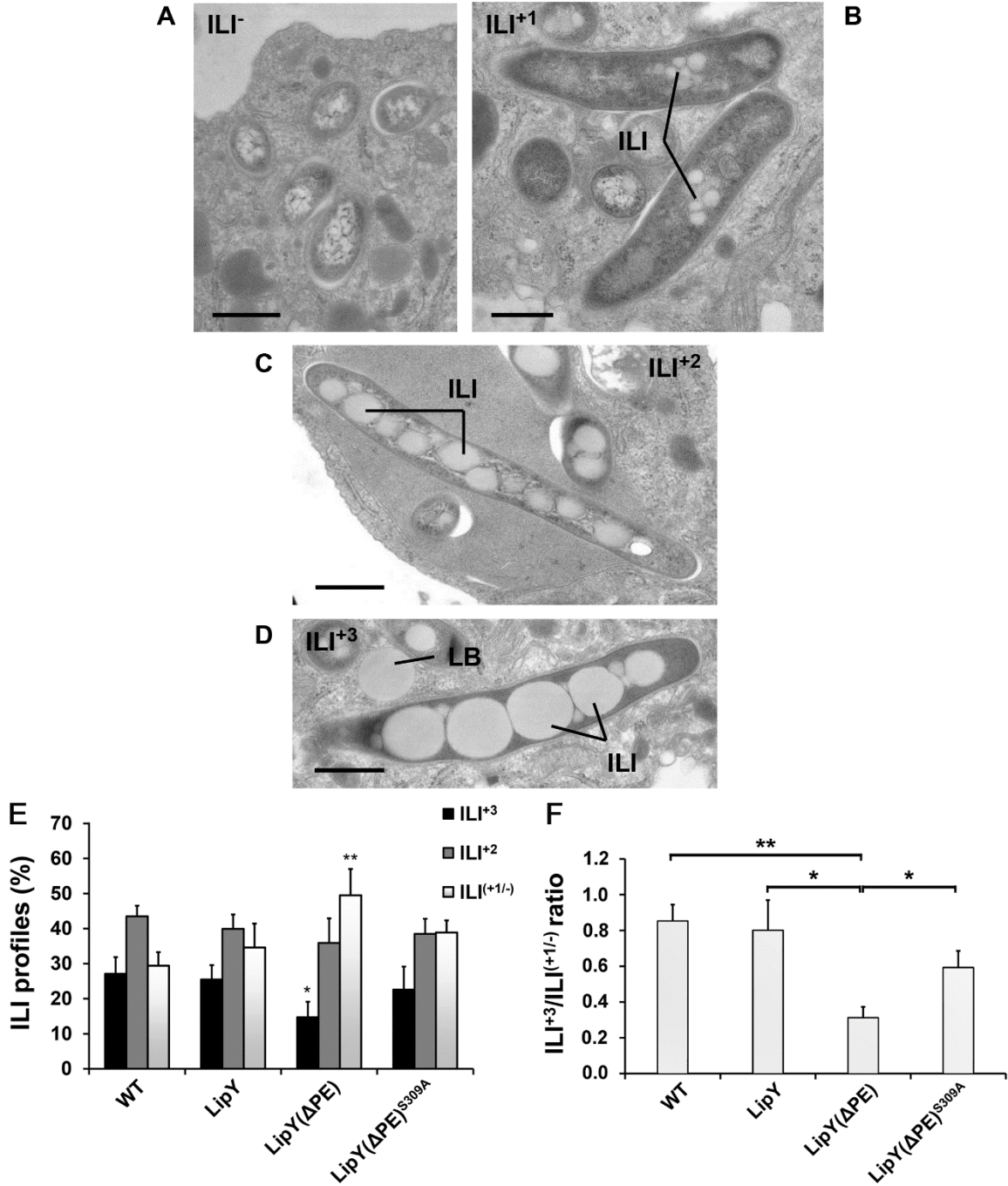


Figure 4

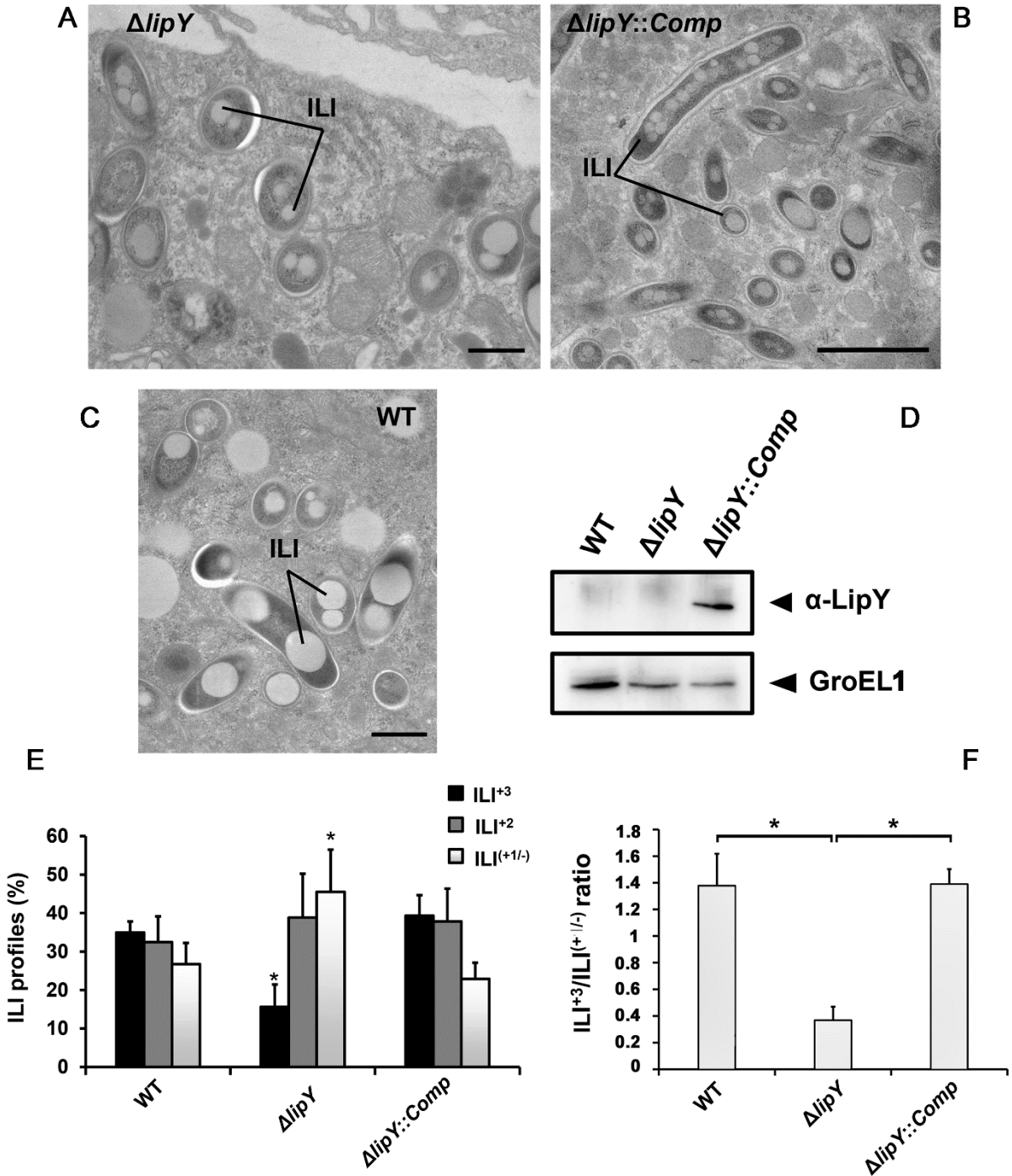


Figure 5

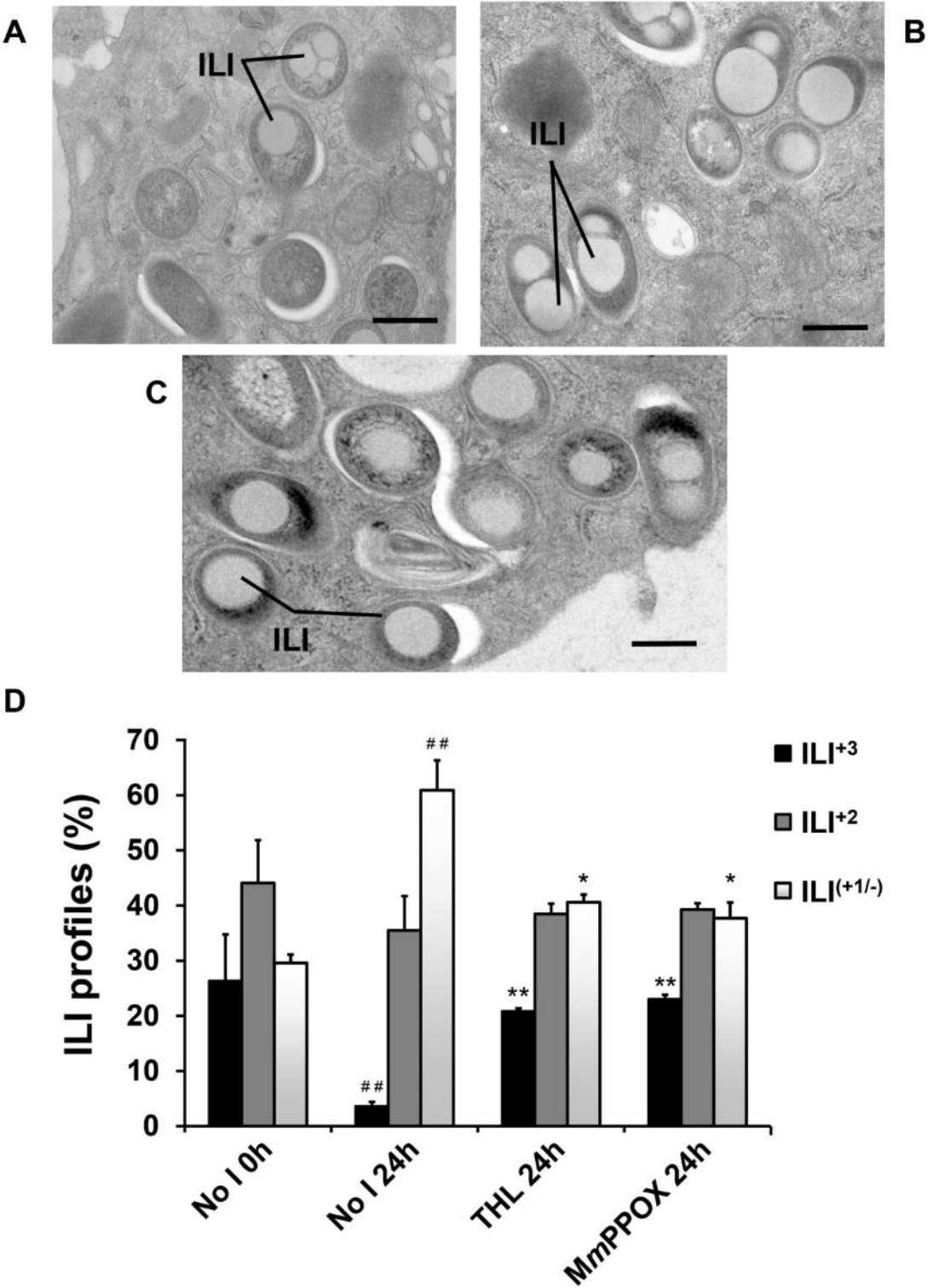


Figure 6

